

NACA RM E57D15

7012

~~CONFIDENTIAL~~

Copy 267  
RM E57D15

5122

0149730

TECH LIBRARY KAFB, NM

NACA

# RESEARCH MEMORANDUM

AERODYNAMIC PERFORMANCE OF SEVERAL TECHNIQUES FOR  
SPIKE-POSITION CONTROL OF A BLUNT-LIP NOSE INLET  
HAVING INTERNAL CONTRACTION; MACH NUMBERS  
OF 0.63 AND 1.5 TO 2.0

By Arthur A. Anderson and Maynard I. Weinstein

Lewis Flight Propulsion Laboratory  
Cleveland, Ohio (Unclassified)

Classification cancelled (or changed to) .....  
By Authority of NASA Tech Pub. Announcement #32  
(OFFICER AUTHORIZED TO CHANGE)

By ..... 24 Nov 60 .....

..... NK .....  
GRADE OF OFFICER MAKING CHANGE  
13 Feb 61  
DATE CLASSIFIED DOCUMENT

This material contains information affecting the National Defense of the United States within the meaning of the espionage laws, Title 18, U.S.C., Secs. 793 and 794, the transmission or revelation of which in any manner to an unauthorized person is prohibited by law.

## NATIONAL ADVISORY COMMITTEE FOR AERONAUTICS

WASHINGTON

September 17, 1957

~~CONFIDENTIAL~~



0143930

## NATIONAL ADVISORY COMMITTEE FOR AERONAUTICS

RESEARCH MEMORANDUM

AERODYNAMIC PERFORMANCE OF SEVERAL TECHNIQUES FOR SPIKE-

POSITION CONTROL OF A BLUNT-LIP NOSE INLET

HAVING INTERNAL CONTRACTION; MACH

NUMBERS OF 0.63 AND 1.5 TO 2.0

By Arthur A. Anderson and Maynard I. Weinstein

## SUMMARY

A study was made to determine locations of pressure sensors for controlling the spike position of a blunt-lip, axisymmetric inlet having internal contraction. The inlet performance was determined at Mach numbers of 0.63 and 1.5 to 2.0 for airflow schedules corresponding to those of a given turbojet engine over a wide range of ambient temperatures.

The use of the ratio of a throat static pressure to either a local total or the spike-tip total pressure provided a signal that could set nearly maximum pressure recoveries at Mach numbers of 1.7 to 2.0 and within 6 percent of maximum recovery at Mach 1.5.

For one specific airflow schedule at zero angle of attack, the ratio of throat static pressure to spike-tip total pressure indicated a spike setting that would result in a thrust minus drag within  $1\frac{1}{2}$  percent of the maximum at Mach numbers from 1.5 to 2.0.

The maximum pressure recoveries were 0.90, 0.945, and 0.96 at Mach numbers of 2.0, 1.8, and 1.5, respectively.

## INTRODUCTION

To obtain optimum performance of a supersonic powerplant installation over a wide range of flight Mach numbers, some form of variable inlet geometry usually must be employed. One such form is that of a translating spike (refs. 1 and 2). However, the use of variable geometry requires that, for optimum performance, some means of controlling the spike position must be found. References 3 and 4 present control systems

~~CONFIDENTIAL~~~~CONFIDENTIAL~~

using shock position to define the operating point for inlets without internal contraction. The controlling action was accomplished by sensing the pressure rise across a normal shock and thereby positioning the spike to maintain the shock at the sensor station (at the cowl lip).

On spike inlets with excessive internal contraction, the normal-shock position is ahead of the cowl lip at critical flow and may vary so widely with flight Mach number and ambient temperature that it is difficult to use a single shock-positioning probe or orifice to maintain maximum inlet performance (which generally occurs near critical flow). An Air Force contractor proposed that the pressure rise at the throat with subcritical operation could be used to provide the spike-positioning signal that would maintain an internal contraction inlet at critical flow. This investigation was made to study such a control technique, using a blunt lip, over-contracted inlet with a remotely controllable 25° half-angle spike. The study was directed towards finding the internal location of the pressure measuring stations that would provide suitable control signals. Also included was an evaluation of the pressure recovery, drag, and stability of the inlet at Mach numbers of 0.63 and 1.5 to 2.0. Although data were taken at angles of attack from 0° to 10°, the greater part was taken at 3°. The study was conducted in the NACA Lewis 8- by 6-foot supersonic wind tunnel at a Reynolds number of about  $5 \times 10^6$  per foot.

#### SYMBOLS

A	area
$A_c$	inlet capture area (vertical tangent at lip), 0.323 sq ft
$A_2$	flow area at the compressor-face station, 0.284 sq ft
$C_D$	drag coefficient based on frontal area of 0.535 sq ft
D	full-scale pressure plus additive drag, lb
F	engine net thrust, lb
$M_0$	free-stream Mach number
$\frac{m_2}{m_0}$	mass-flow ratio, $\frac{\rho_2 V_2 A_2}{\rho_0 V_0 A_c}$
P	total pressure
p	static pressure

CG-1 back

$\Delta P$	difference between maximum and minimum total pressure at engine-face rake
$\Delta P/P_2$	distortion parameter
$V$	velocity
$\frac{w\sqrt{\theta}}{\delta A}$	corrected airflow rate per unit area, lb/(sec)(sq ft)
$w$	airflow rate, lb/sec
$\alpha$	angle of attack, deg
$\delta$	ratio of total pressure to NACA standard sea-level pressure of 2116 lb/sq ft
$\theta$	ratio of total temperature to NACA standard sea-level temperature of 518.7° R
$\theta_2$	spike-position parameter (angle between inlet centerline and a line from the spike tip to the vertical tangent at the cowl lip)
$\rho$	density
Subscripts:	
a,b,c,d,e	pressures shown in fig. 3
1	ideal
0	free stream
2	compressor-face location (20.6 in. from cowl lip)

## APPARATUS AND PROCEDURE

### Model Details

The quarter-scale translating-spike inlet model, schematically shown in figure 1(a), was strut-mounted from the support sting. Airflow through the inlet was varied with a remotely controlled plug. As shown in figure 1(b), the translating portion of the centerbody consisted of a 25° half-angle conical spike that was faired into a cylindrical section. The spike position was remotely variable.

Figure 1(c) shows the geometric details of the rounded-lip cowl; the axial reference station for the cowl coordinates is the vertical tangent at the cowl lip. Also shown in this figure are the locations of the static-pressure orifices from which the cowl drags were computed; the model did not include a force balance.

The diffuser-area variation for various spike settings is shown in figure 2. As shown in the sketch, the spike-position parameter  $\theta_i$  is the angle between a line from the spike tip to the vertical tangent at the cowl lip and the model centerline. The maximum spike-position parameter position ( $63.6^\circ$ ) represents the spike fully retracted for flight at subsonic and low supersonic speeds.

A number of inlet rakes that included static- and total-pressure probes were installed near the throat to study pressure variation with spike translation that could provide signals for spike-position control. Examination of the data from these rakes showed that the most promising control signals could be provided by the rake shown in figure 3. Data from this particular rake only are presented in the report. The rake was mounted inside the cowl in the horizontal plane and included one pitot and one pitot-static probe. Ratios of pressures that are discussed in the report in terms of control performance are designated A, B, C, and D and are shown in figure 3.

Mass flow through the inlet was computed from the measured static pressure at a station 34.0 inches downstream of the cowl lip (fig. 1(a)) with the assumption of isentropic flow to the known area at the choked exit. Total-pressure recovery was obtained from the averaged readings of 40 total-pressure probes located at the centroids of equal flow area at station 2, the full-scale compressor-face station. The inner and outer radii of the tubes used for computing distortions were, respectively, 37 and 95 percent of the maximum radius at station 2. (The hub-tip ratio at that station was 0.32.) A dynamic-pressure transducer located just downstream of station 2 was used with a recording oscillograph in determining the inlet instability characteristics.

#### Procedure

The experimental data were obtained by translating the spike while simulating given engine airflows with fixed positions of the exit plug. The airflow schedules of the engine for which the inlet was designed are shown in figure 4. (A constant of  $2.3 \text{ lb}/(\text{sec})(\text{sq ft})$  for auxiliary air has been added to the engine values in order to simulate properly the total full-scale flow into the inlet.) Data were taken to include the three airflow schedules shown:

(a) Air Force standard cold day above 56,800 feet

(b) NACA standard day above 35,332 feet

(c) A structural-limit condition in which the total temperature at the compressor face is limited to  $710^{\circ}$  R. At Mach number 2.0, this airflow corresponds to the NACA standard day, but in the lower flight Mach number range (1.7 and below), this curve follows the Air Force standard day. The airflow settings from Mach numbers of 1.8 to 1.9 do not correspond to any "day" condition, but are intermediate between the NACA standard day and the Air Force hot day atmospheres.

The major portion of the data was obtained at  $3^{\circ}$  angle of attack, the design cruise attitude of the nacelle. Limited data were obtained at  $0^{\circ}$ ,  $6^{\circ}$ , and  $10^{\circ}$  angles of attack.

## RESULTS AND DISCUSSION

### Inlet Performance

Inlet performance characteristics (total-pressure recovery and distortion, mass flow, and drag) at Mach numbers of 2.0, 1.8, and 1.5 are shown, respectively, in figures 5, 6, and 7 as a function of the spike-position parameter for the airflow conditions given in figure 4. Total-pressure distortions were computed by dividing the difference between maximum and minimum pressures at the rake station by the average total pressure. On the pressure-recovery curves, critical flow is indicated by an arrow; supercritical operation is to the left of the arrow, subcritical is to the right. These performance regions are also indicated on the mass-flow plots. Here the dashed lines on the figures are the supercritical (or maximum) mass-flow ratios as obtained by varying the spike position with the control plug at the wide-open position. The difference between the data points and the dashed line thus represents the subcritical spillage within the accuracy of the mass-flow data.

Cowl pressure drags were obtained by a pressure-area integration between the limits of (1) the assumed stagnation point on the lip and (2) the maximum cowl diameter. (With the instrumentation available, drags could be computed for zero angle of attack only and hence form a limited portion of the data.) The summation of pressure drag and additive drag is also given in the drag plots of figures 5 to 7. Additive drag was computed by the techniques given in reference 5.

In brief, the basic supersonic performance without engine-matching considerations may be summarized as follows:

CONFIDENTIAL

(1) At low angles of attack, total-pressure distortions near critical flow generally were on the order of 10 percent and tended to increase on either side of critical flow. In a few instances, distortions at critical flow were as high as 20 percent.

(2) Maximum pressure recoveries at zero angle of attack were 0.90, 0.945, and 0.96 at Mach numbers of 2.0, 1.8, and 1.5, respectively. In general, peak recoveries occurred with the inlet slightly subcritical.

(3) Maximum mass-flow ratios were 0.89, 0.81, and 0.74 at Mach numbers of 2.0, 1.8, and 1.5, respectively. At the two higher Mach numbers, retracting the spike gave a peaked curve of mass-flow ratio because of the decreased oblique-shock spillage and then the subsequent overriding spillage due to the internal contraction (see diffuser area, fig. 2).

(4) Minimum (cowl pressure plus additive) drag coefficients were 0.15, 0.20, and 0.23 at Mach numbers of 2.0, 1.8, and 1.5, respectively. These values are appreciably higher than those reported in reference 6 for an inlet having the same lip shape (and a capture area about 10 percent smaller). The differences result mainly from the fact that the greater number of orifices on the present inlet permitted a more accurate integration of cowl pressures.

Subsonic mass-flow pressure-recovery characteristics of the inlet (Mach 0.63) are shown in figure 8 for four spike positions including the fully retracted case. Subcritical pressure recoveries were above 95 percent and essentially independent of spike position; critical mass flow increased with spike retraction because of the increase in throat area. At maximum spike retraction (spike-position parameter,  $63.6^\circ$ ) the corrected airflow at critical inlet operation (37 lb/(sec)(sq ft)) corresponds to an ambient temperature of about  $110^\circ\text{F}$ ; any lower temperature results in supersonic matching. As shown in figure 8, the supersonic matching for the NACA standard day conditions above 35,332 feet results in a loss in recovery of about 10 percentage points below the critical value.

#### Engine-Inlet Matching Considerations

The variation of the thrust-minus-drag parameter with spike position is shown in figure 9 for airflows where drag data were available (i.e., at zero angle of attack for (1) the NACA standard day at Mach numbers of 1.5 to 2.0 and (2) at Mach number 1.8, the structural limit and Air Force cold day). The spike positions for peak and critical pressure recovery and minimum drag (from figs. 5 to 7) are marked by arrows on the curves. At any Mach number and ambient temperature, the spike should be set at the position for maximum thrust-minus-drag performance. However, because of the limited amount of drag data, most of the control data of

this report will be presented with regard to the ability to set maximum pressure recovery. Justification for this expedient is shown in figure 9 by the fact that peak pressure recoveries and minimum drags occur very near to each other and very near to the maximum value of the thrust-minus-drag parameter.

A summary of the peak pressure recoveries for the three airflow schedules is shown in figure 10 for Mach numbers of 1.5 to 2.0 at an angle of attack of  $3^\circ$ . For the structural-limit and NACA-standard-day schedules, peak pressure recoveries are generally well above 0.90 but, for the Air Force cold day temperatures, the peak values are only 0.83 to 0.88. These poor recoveries at the low temperature emphasize the difficulty of sizing an inlet for high performance over a wide range of ambient temperatures (ref. 7). The problem can be further illustrated by the following table, which compares inlet operating conditions (at peak recovery) for the extremes of ambient temperature at Mach number 2.0. (Data are from fig. 5(b).)

"Day"	Corrected airflow rate, $\left(\frac{w\sqrt{\theta}}{8A}\right)_2$ , lb/(sec)(sq ft)	Mass-flow ratio, $\frac{m_2}{m_0}$	Total pressure recovery, $\frac{P_2}{P_0}$	Spike-position parameter, $\theta_1$ , deg
NACA standard	30.7	0.82	0.90	38.5
Air Force cold	36.1	.89	.83	41.0

Although the mass flow is increased at the lower temperature, the inlet is not large enough to avoid the reduction in pressure recovery necessary

to supply the larger corrected weight flow  $\left[\frac{m_2/m_0}{P_2/P_0} = f\left(\frac{w\sqrt{\theta}}{8A}\right)_2\right]$ . Data are available to make a comparison in terms of thrust minus drag at a Mach number of 1.8; the penalties incurred at the lower temperature are shown in figure 9. The larger inlet that would be required to improve the low-temperature operation would, of course, penalize performance at higher temperatures because of the greater spillages required.

#### Stability

The effect of spike translation on inlet stability is shown in figure 11 for angles of attack  $0^\circ$ ,  $3^\circ$ , and  $6^\circ$  at a Mach number of 2.0, and for angles of attack  $0^\circ$  and  $3^\circ$  at Mach numbers of 1.8 and 1.5. Two stability boundary lines are shown at each angle of attack, one for no oscillation (start of pulsing) and the other for half-amplitude static pressure fluctuations at the diffuser exit equal to  $2\frac{1}{2}$  percent of the



free-stream total pressure. The data were obtained by forcing the inlet far into the instability region at a given spike position and then increasing the weight flow until stable flow was reached. The minimum matching airflow for each Mach number is shown as the upper horizontal line on each set of curves; airflows below this line are outside the normal operating region of the inlet. Thus, if half amplitudes greater than  $\frac{1}{2}$  percent of the free-stream total pressure are arbitrarily called buzz, the inlet would appear to be buzz-free at all Mach numbers for angles of attack below  $3^\circ$ . At a Mach number of 2.0, buzz could occur at  $6^\circ$  angle of attack for values of the spike-position parameter less than about 43.5°. (Peak pressure recovery occurs at  $40^\circ$ .)

### Schlieren Photographs

Schlieren photographs of critical inlet operation at  $3^\circ$  angle of attack are presented in figure 12 for the three engine airflow schedules. A wide range of normal-shock positions with Mach number and weight flow is shown near critical flow. The variation in normal-shock position with spike retraction for NACA standard day at Mach number 2.0 (fig. 13) shows the increase in normal-shock spillage that accompanies a decrease in oblique-shock spillage.

### Flow Contours at Engine Face

Total-pressure contours at the engine-face station are shown in figure 14 at critical flow for the three engine flow schedules at  $3^\circ$  angle of attack. The distortions at this angle of attack were primarily radial. The tendency for the distortion to increase at a given Mach number with an increase in corrected weight flow (decrease in ambient temperature) may be attributed to the entrance into the inlet of the oblique-normal shock vortex sheet (schlieren, fig. 12) and to the higher Mach numbers at the engine face.

### Spike Control Systems

As previously discussed, the maximum thrust-minus-drag performance at any Mach number and ambient temperature is obtained with the spike at a position close to that for peak pressure recovery. The schlieren views in figure 12 indicate that a single shock sensing probe could not be used to set the spike for critical flow (nor peak pressure recovery) because of the wide range of normal-shock positions at the critical flow. This problem does not exist for inlets without internal contraction; the normal shock passes the cowl lip at critical flow and, hence, a cowl-mounted sensor can be used to set critical, or any degree of subcritical,

flow (refs. 3 and 4). Thus, for inlets with excessive internal contraction, other techniques for spike-position control must be explored. In the present study, the functioning of the control was based on the following approach:

When the internal flow contraction is too great for flow-starting (fig. 2), the throat Mach number is 1.0 at critical flow and decreases as the spike retracts to the subcritical positions. For started-flow conditions, the throat Mach number at critical flow is slightly greater than 1.0. In either case (started or not), the ratio of throat static to total pressure rises from a value of about 0.528 as the spike retracts from the critical flow position, regardless of the location of the normal shock. Thus, the possibility exists that the desired subcritical spike positions can be set over a wide range of flight conditions by maintaining a given throat pressure ratio somewhat greater than 0.528. In addition to forming a ratio with local total pressure, the throat static pressure could be used as a ratio with, for example, the spike static pressure near the tip or the spike-tip total pressure.

With such a control technique, it is necessary to try experimentally a number of positions and types of static- and total-pressure sensors with a given inlet, since: (1) the throat position varies with spike positions; and (2) large static- and total-pressure gradients can exist near the inlet throat, especially at angle of attack. The two types of pressure ratio reported in the following sections are: (1) throat static pressure to local total pressure, and (2) throat static pressure to spike-tip total pressure.

Ratio of static to total pressure at throat. - The throat rake which provided the throat pressure data of this report is shown in figure 3. Ratios A and B, formed from two cowl static pressures and two rake total pressures, are also shown in the figure. The variation of ratio A with spike position is given in figure 15. Here the characteristic rise with subcritical operation (increasing spike-position parameter) is shown. Marked on the abscissa are the angles at which the maximum pressure recoveries occur (figs. 5 to 7). Measured pressure ratios higher than a given value to be used as a control would call for forward movement of the spike and vice versa.

The performance of the inlet with a value of 0.63 for control pressure ratio A (corresponding to a local Mach number of 0.84) is shown in figure 16(a) as a function of free-stream Mach numbers from 1.5 to 2.0. The ordinate is the pressure recovery that would be set by the control, expressed as the percent of the maximum pressure recovery obtainable at that Mach number, weight flow, and angle of attack. (Fig. 10 summarizes these maximum values for  $3^\circ$  angle of attack.) The value of 0.63 showed the most promising control action for pressure ratio A in terms of pressure recovery. By using this pressure ratio at the angles of attack

~~CONFIDENTIAL~~

investigated for the three airflow schedules, it is shown in figure 16(a) that a control system could set the maximum available pressure recoveries at Mach numbers from 1.7 to 2.0, and that, at a Mach number of 1.5, pressure recoveries would be within 94 percent of the maximum values.

Figure 16(a) also shows that the control performance at the lower Mach numbers could be improved over that of ratio A by using closer to the throat a static-pressure sensing station that moves downstream with the spike retraction required at the lower Mach numbers. Thus, near-maximum pressure recovery is indicated at Mach numbers 1.5 and 1.6 by use of ratio C (fig. 3), formed from a static-pressure value measured 3.35 inches from the lip (the throat is about 4 in. downstream of the lip at Mach number 1.5, as shown in fig. 2). However, the performance above Mach number 1.6 with ratio C (not shown) drops sharply so that good performance over the entire Mach number range could be obtained only by adding control circuits for switching the sensing pressures at about Mach number 1.7.

Inlet performance is given in figure 16(b), with a value of 0.60 for control pressure ratio A, to show the sensitivity to less-than-optimum pressure ratio, that is,  $A = 0.63$ . Poorer performance (compared with that of fig. 16(a)), by 1 to 2 percent of the maximum available pressure recovery, is shown over most of the Mach number range.

The pressure recoveries that would be provided by use of the optimum value (0.61) of ratio B are presented in figure 17. Essentially, the performance is the same as that for the best value of ratio A (fig. 16(a)) except for the Air Force cold day conditions, where the recovery is slightly less at Mach number 2.0 and somewhat better at the lower Mach numbers. Pressure-recovery sensitivity to less-than-optimum values of ratio B was similar to that shown for ratio A.

Ratio of throat static pressure to spike-tip total pressure. - The ratio of the internal static pressure  $c$  (fig. 3) to the total pressure at the spike tip is designated as control ratio D, which, at a value of 0.70, indicated generally better pressure recoveries (fig. 18) than those obtained with ratios A or B. Pressure recoveries were within 1 percent of the maximum available for all conditions except the NACA standard day and Air Force cold day at Mach number 1.5, where a loss of generally less than 3 percent is shown.

Thrust-minus-drag performance. - Inlet performance with ratios A and D as sensing signals is shown in figures 19(a) and (b), respectively, in terms of  $\frac{F - D}{F_1}$ , the net thrust parameter. Data are presented for zero angle of attack at the NACA standard day flight conditions. Values of the net thrust parameter set by the control signals are compared with the maximum obtainable values of the parameter (fig. 9). Maximum performance is attained with ratio A at Mach numbers of 1.8 and 2.0 (fig. 19(a)). For this ratio, data were not available at Mach number 1.5 for

~~CONFIDENTIAL~~

zero angle of attack but, based on the pressure recoveries at an angle of  $3^\circ$ , the net thrust would fall well below the maximum at that Mach number. The control settings with ratio D (fig. 19(b)) indicate performance within  $1\frac{1}{2}$  percent of the maximum thrust minus drag over the entire 1.5 to 2.0 Mach number range.

#### SUMMARY OF RESULTS

A translating-spike inlet having a blunt lip and internal contraction was studied to determine the location of sensors usable for spike-position control over a wide range of engine airflows. The following observations can be made from the data:

1. Suitable control signals apparently might be supplied by static pressure near the throat used as a ratio either with a local total pressure or with the spike-tip total pressure.
2. The ratio using the spike-tip total pressure indicated slightly better pressure-recovery performance than the ratio using local total pressure over the Mach number range of 1.5 to 2.0. Both ratios showed promise of setting very nearly the maximum obtainable pressure recoveries at Mach numbers from 1.7 to 2.0 and within 6 percent of maximum recovery at Mach number 1.5.
3. In terms of thrust minus drag, use of the ratio of throat static to spike-tip pressure showed performance within  $1\frac{1}{2}$  percent of the maximum available at Mach numbers from 1.5 to 2.0 for one specific engine airflow schedule at zero angle of attack.
4. The inlet performance without engine-matching considerations showed maximum pressure recoveries of 0.90, 0.945, and 0.96 at Mach numbers of 2.0, 1.8, and 1.5, respectively.

Lewis Flight Propulsion Laboratory  
National Advisory Committee for Aeronautics  
Cleveland, Ohio, June 14, 1957

#### REFERENCES

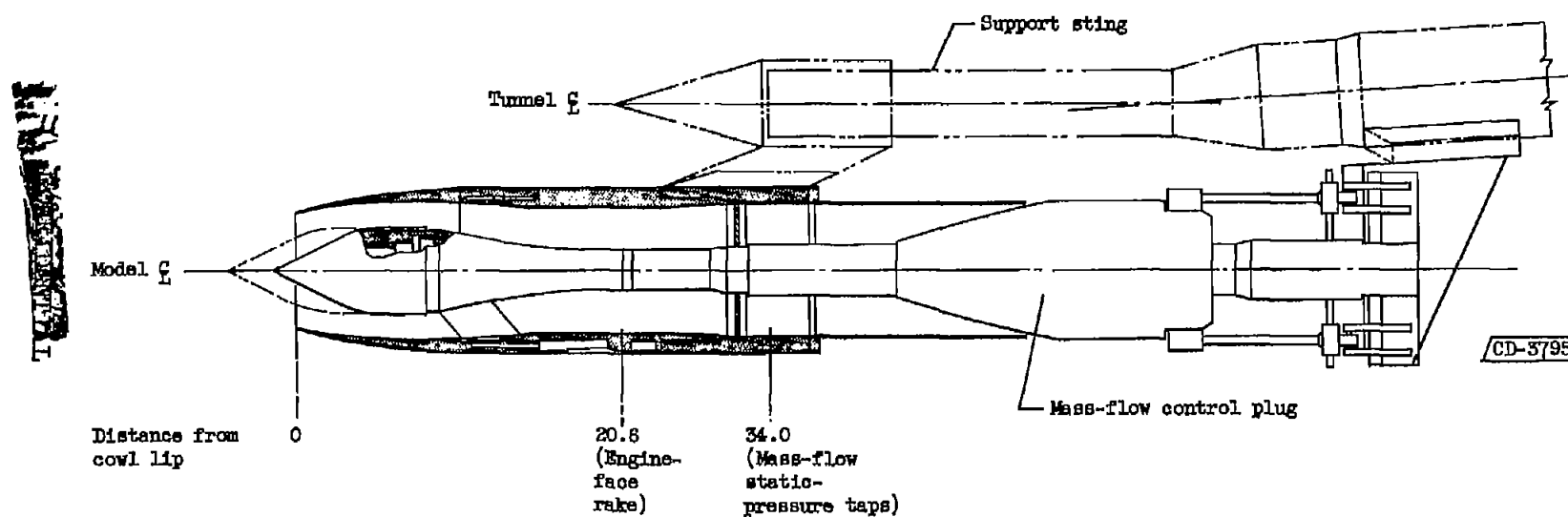
1. Gorton, Gerald C.: Investigation of Translating-Spike Supersonic Inlet as Means of Mass-Flow Control at Mach Numbers of 1.5, 1.8, and 2.0. NACA RM E53G10, 1953.

~~CONFIDENTIAL~~

2. Leissler, L. Abbott, and Sterbentz, William H.: Investigation of a Translating-Cone Inlet at Mach Numbers from 1.5 to 2.0. NACA RM E54B23, 1954.
3. Leissler, L. Abbott, and Nettles, J. Cary: Investigation to Mach Number 2.0 of Shock-Positioning Control Systems for a Variable-Geometry Inlet in Combination with a J34 Turbojet Engine. NACA RM E54I27, 1954.
4. Wilcox, Fred A., and Perchonok, Eugene: Aerodynamic Control of Supersonic Inlets for Optimum Performance. NACA RM E55L14, 1956.
5. Sibulkin, Merwin: Theoretical and Experimental Investigation of Additive Drag. NACA Rep. 1187, 1954. (Supersedes NACA RM E51B13.)
6. Gorton, Gerald C., and Dryer, Murray: Comparison at Supersonic Speeds of Translating Spike Inlets Having Blunt- and Sharp-Lip Cowls. NACA RM E54J07, 1955.
7. Perchonok, Eugene, and Hearsh, Donald P.: Effect of Ambient-Temperature Variation on the Matching Requirements of Inlet-Engine Combinations at Supersonic Speeds. NACA TN 3834, 1957.

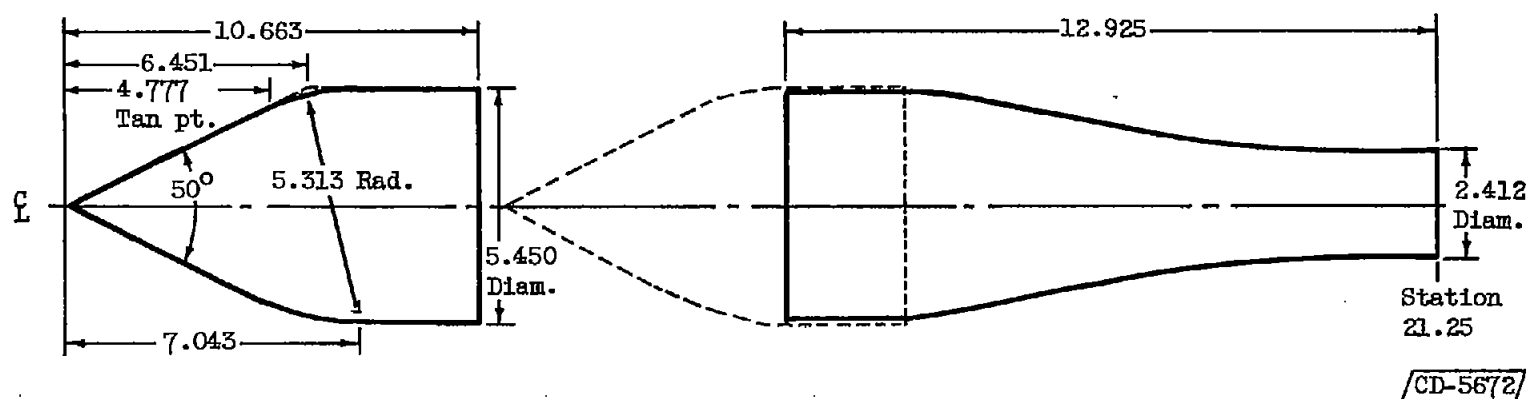
cc13

CONFIDENTIAL



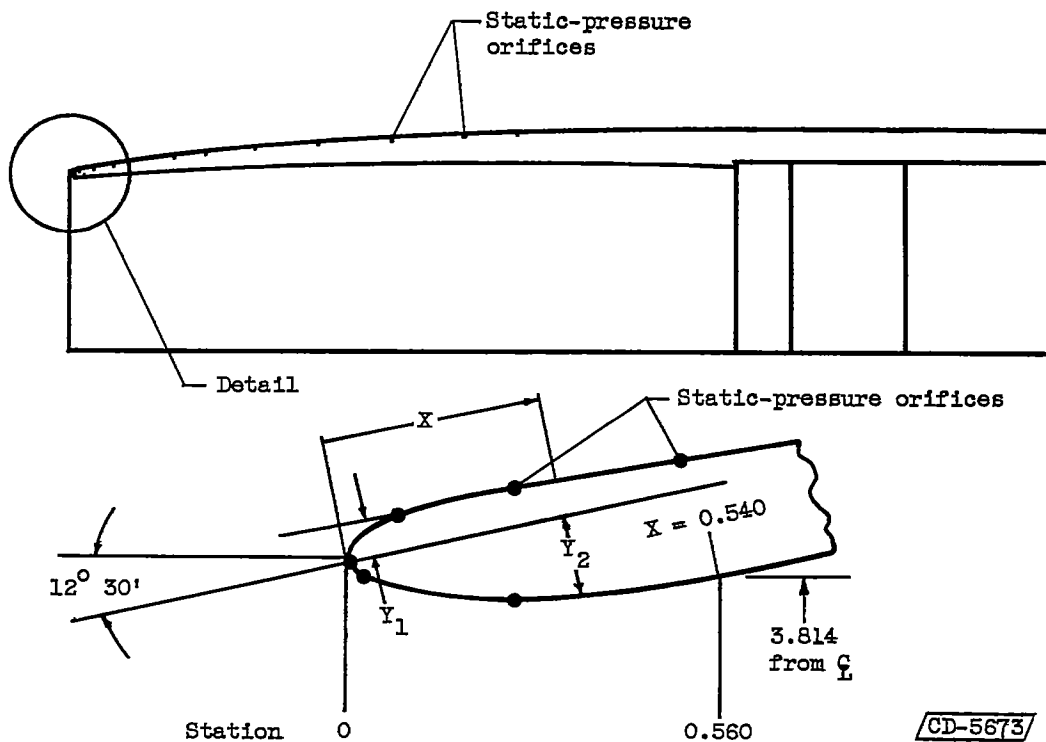
(a) Installation in Lewis 8- by 6-foot supersonic wind tunnel.

Figure 1. - Translating-spike inlet model. (All dimensions in inches.)



(b) Centerbody dimensions.

Figure 1. - Continued. Translating-spike inlet model. (All dimensions in inches.)



Nacelle coordinates		
Station	Outside radius	Inside radius
0.600	4.008	3.823
1.850	4.229	4.010
4.350	4.533	4.182
6.850	4.725	4.274
9.350	4.876	4.354
11.850	4.950	4.235
14.350		4.003
16.850		3.847
19.350		3.804
21.250	4.950	3.800

Lip Coordinates		
X	$Y_1$	$Y_2$
0	0	0
.003	.005	.009
.006	.012	.021
.013	.016	.030
.025	.023	.040
.038	.029	.049
.050	.033	.056
.063	.037	.063
.075	.040	.064
.100	.044	.080
.125	.047	.090
.150	.049	.100
.180	.050	.108
.200		.113
.225	same as	.119
.250	nacelle	.123
.313	geometry	.134
.375		.141
.438		.146
.500		.149
.540		.150

(c) Cowl dimensions

Figure 1. - Concluded. Translating-spike inlet model. (All dimensions in inches.)



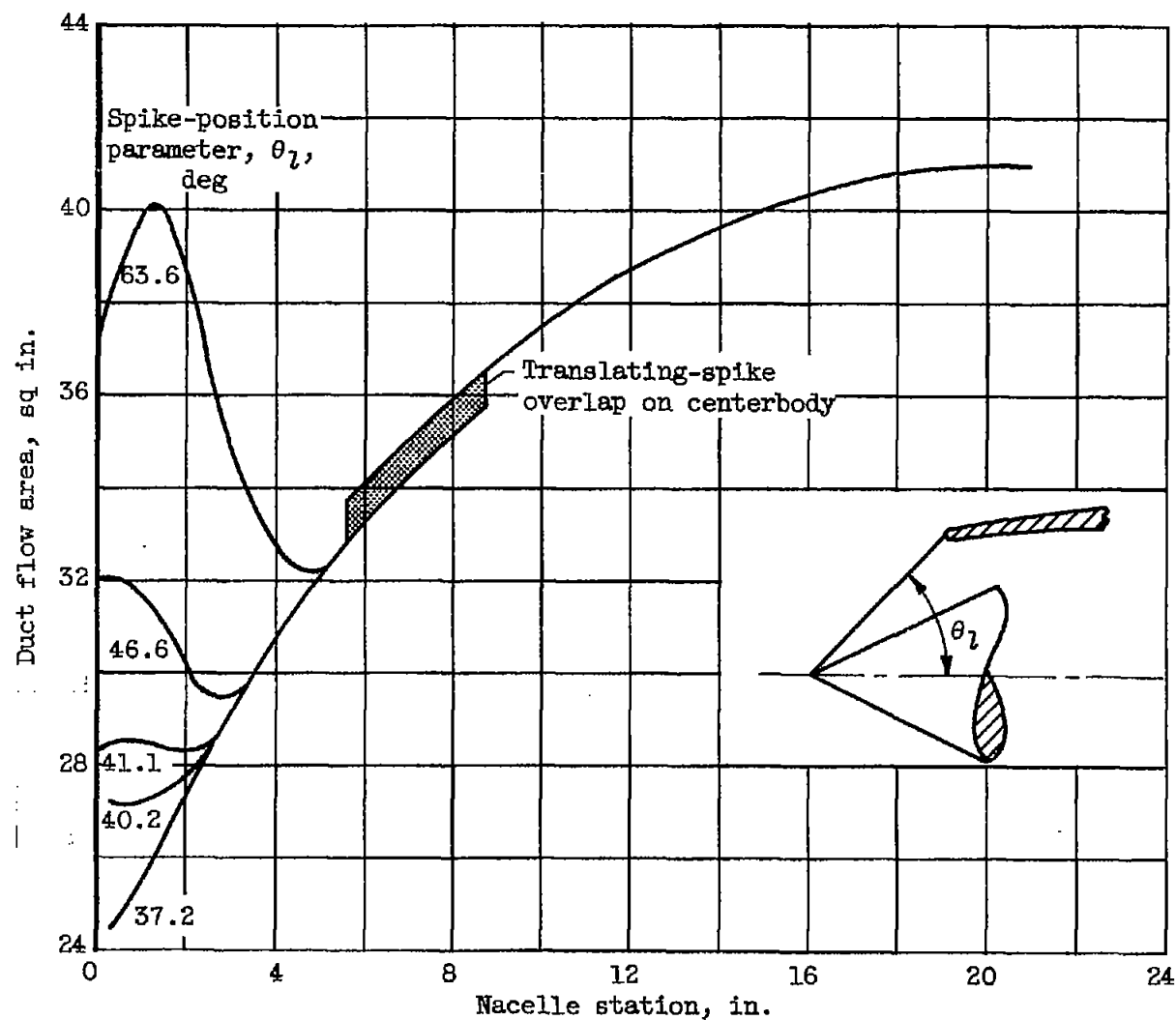
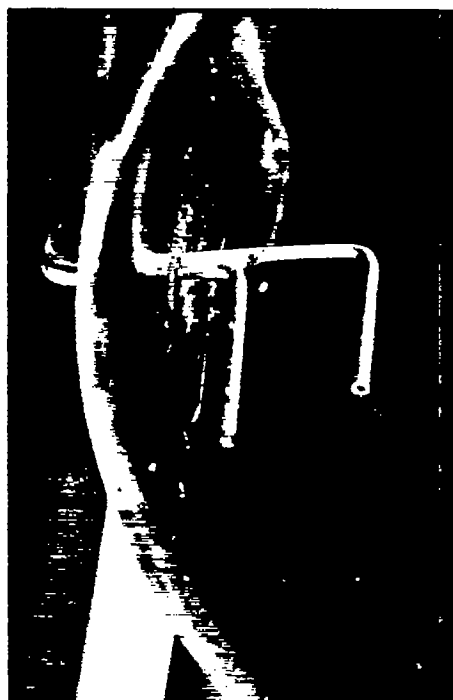
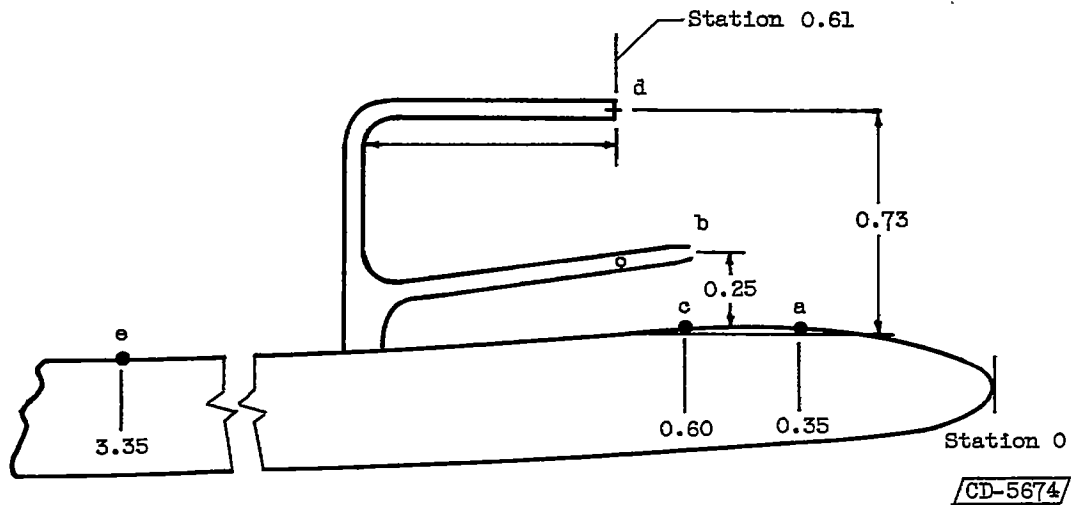


Figure 2. - Diffuser-area variation.

4133

CG-3



C-45218

Ratio	Pressures
A	$p_a/p_b$
B	$p_c/p_d$
C	$p_e/p_b$
D	$p_c/p_f$

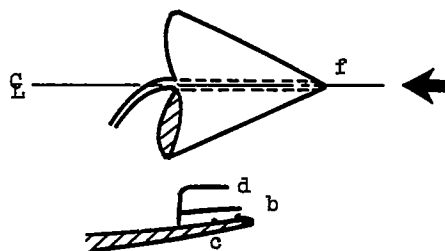


Figure 3. - Throat rake and control pressure ratios. Total pressure,  $P$ ; static pressure,  $p$ . (All dimensions in inches.)

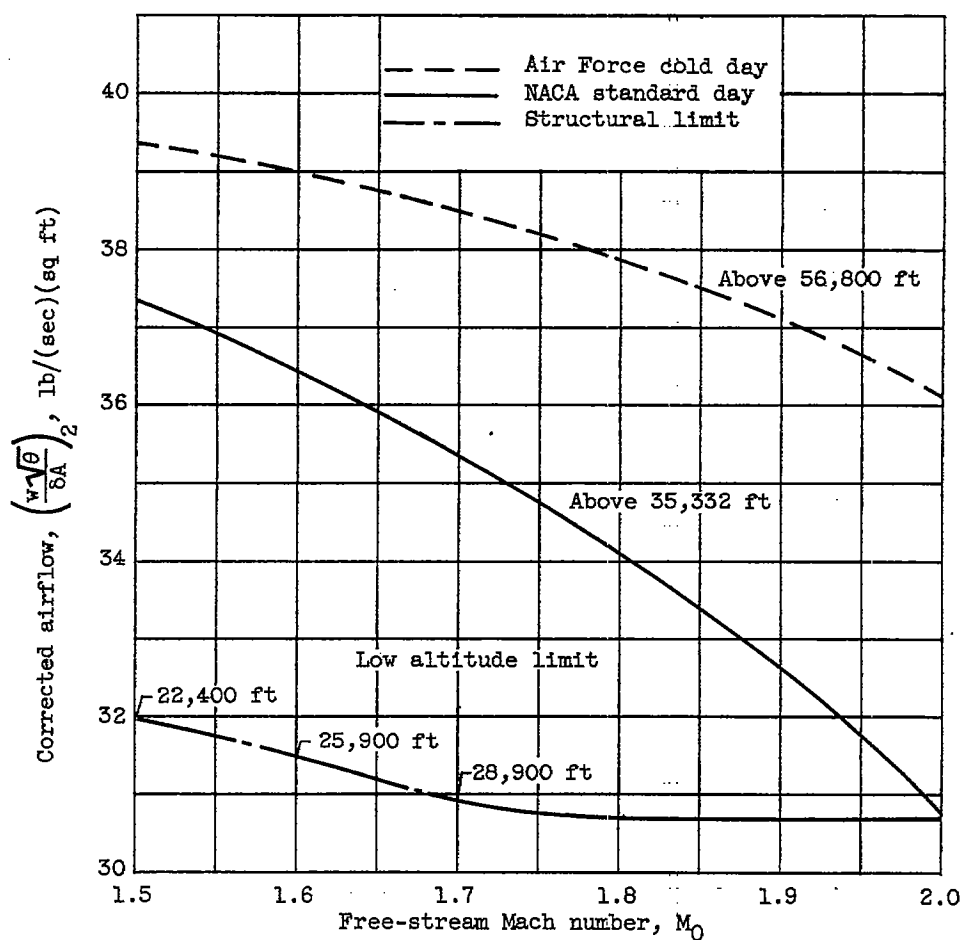


Figure 4. - Schedules of engine-plus-cooling airflows.

CG-3 back 4133

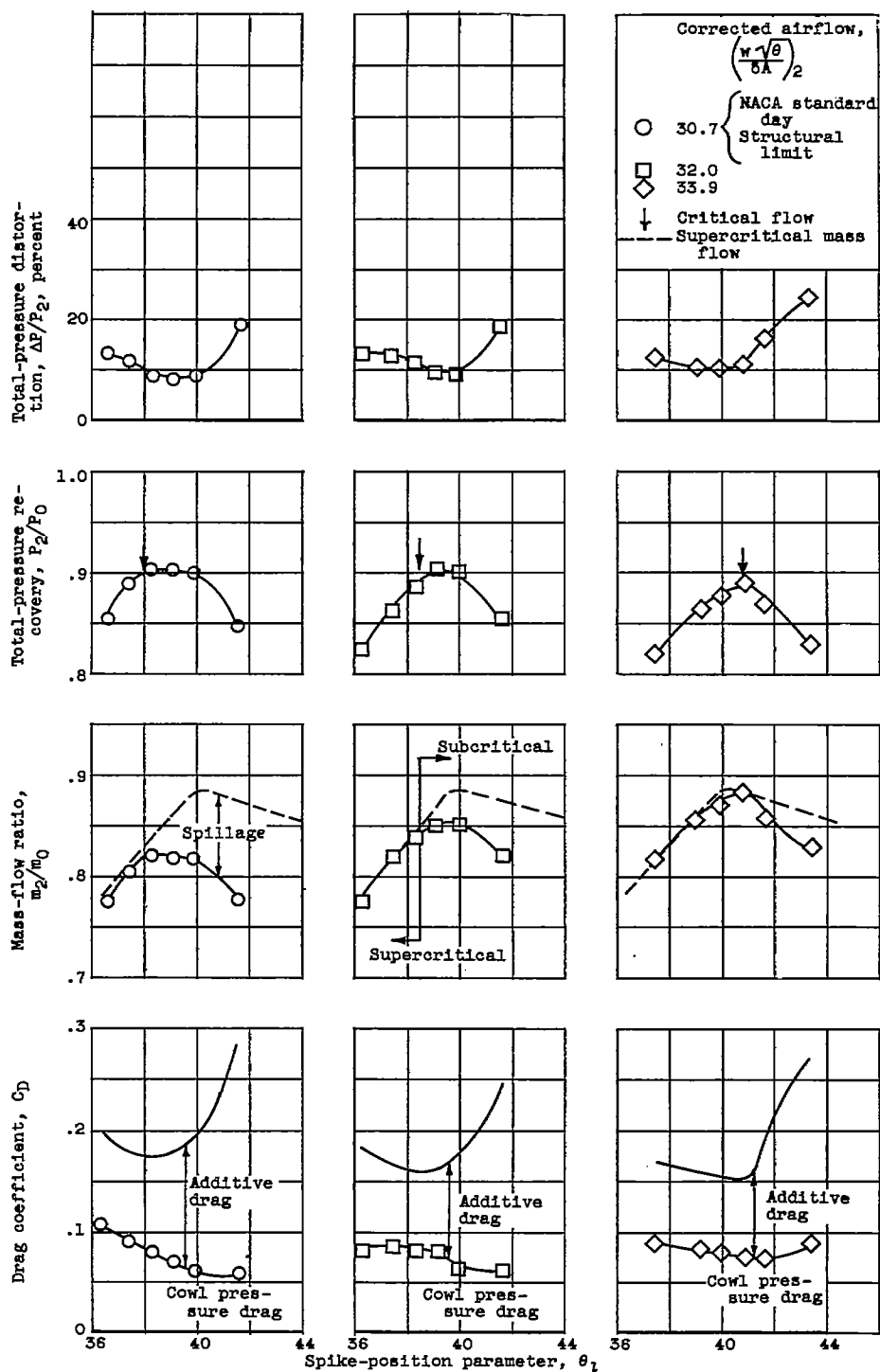
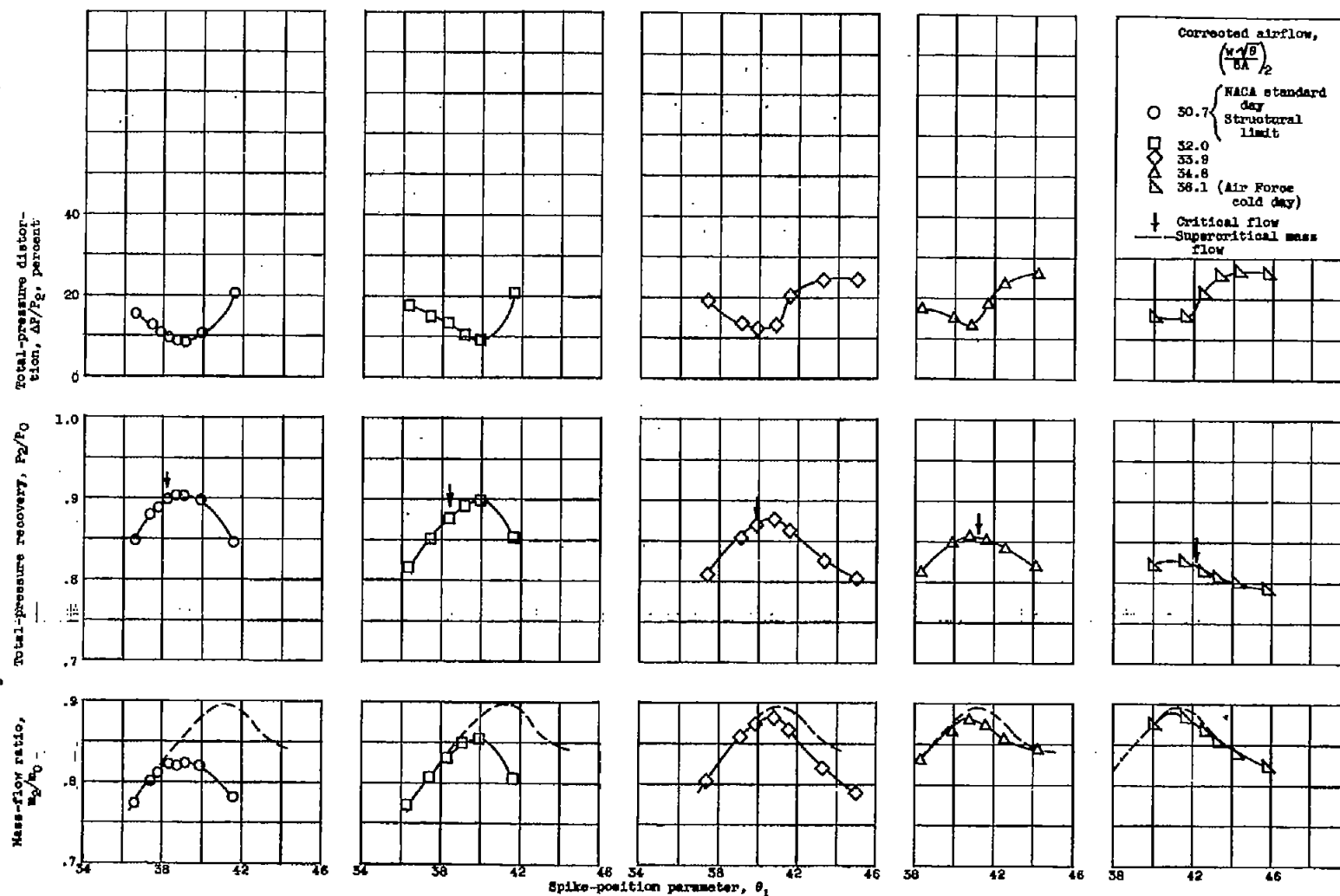
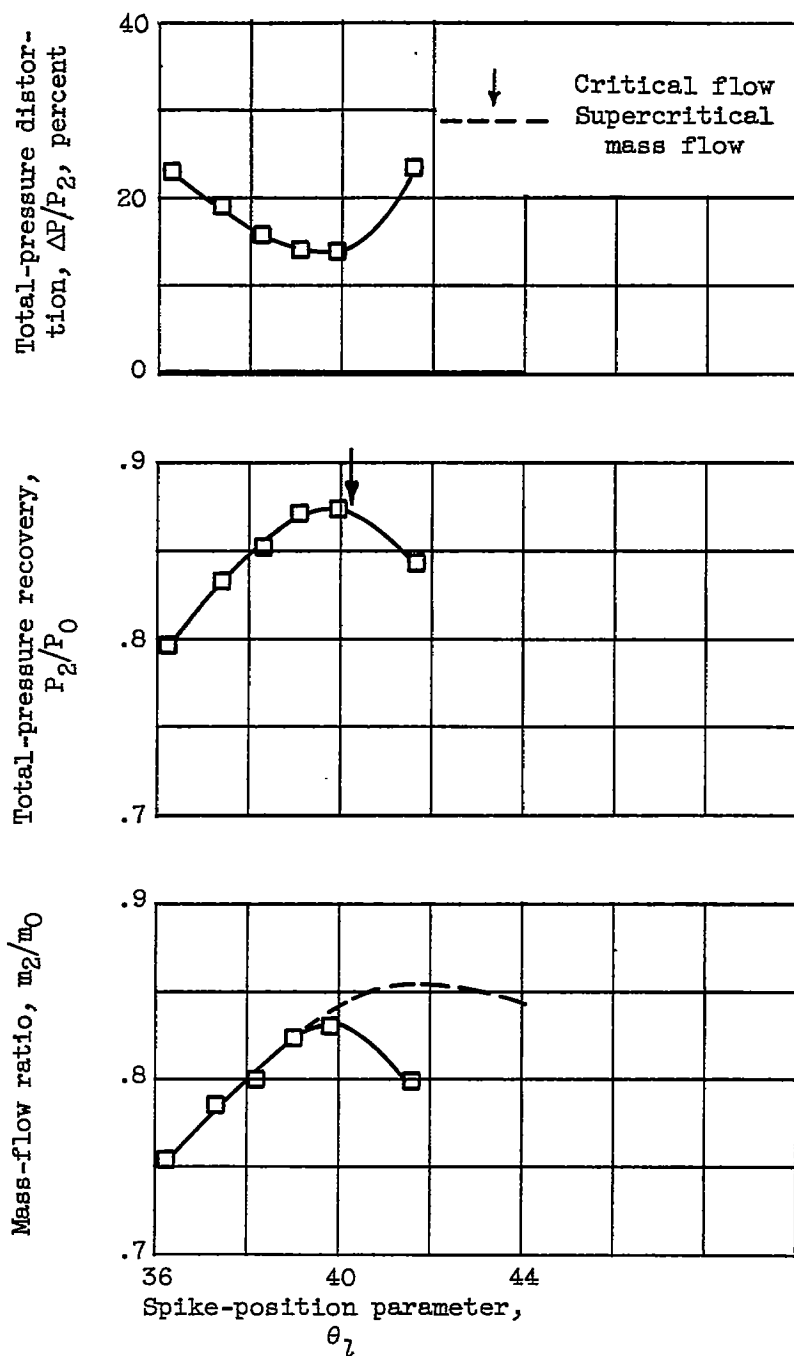
(a) Angle of attack,  $0^\circ$ .

Figure 5. - Inlet performance at free-stream Mach number of 2.0. Shock angle, 42.6°.

(b) Angle of attack,  $3^\circ$ .Figure 5. - Continued. Inlet performance at free-stream Mach number of 2.0. Shock angle,  $42.6^\circ$ .

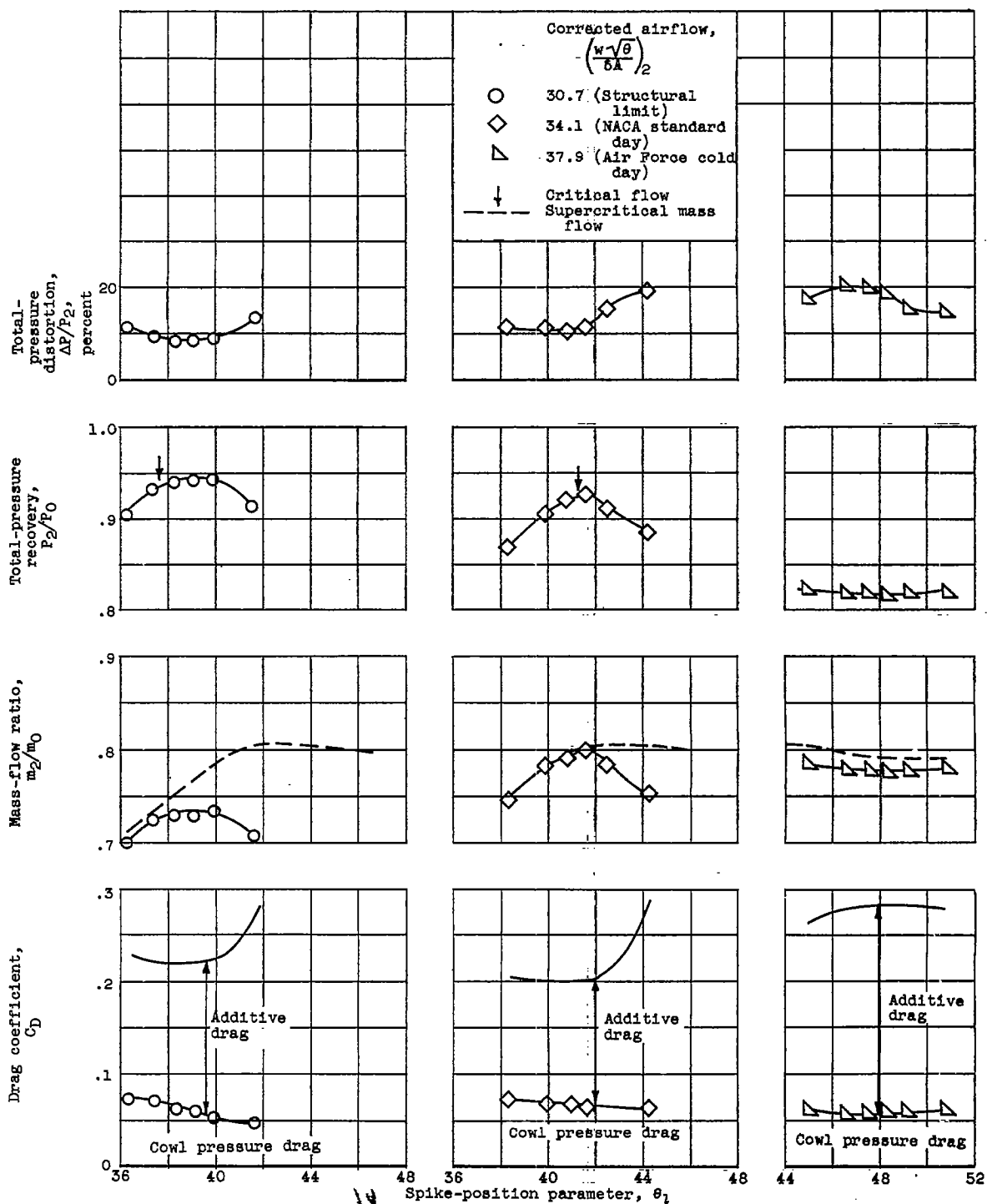


(c) Angle of attack,  $6^\circ$ ; corrected airflow, 32.0.

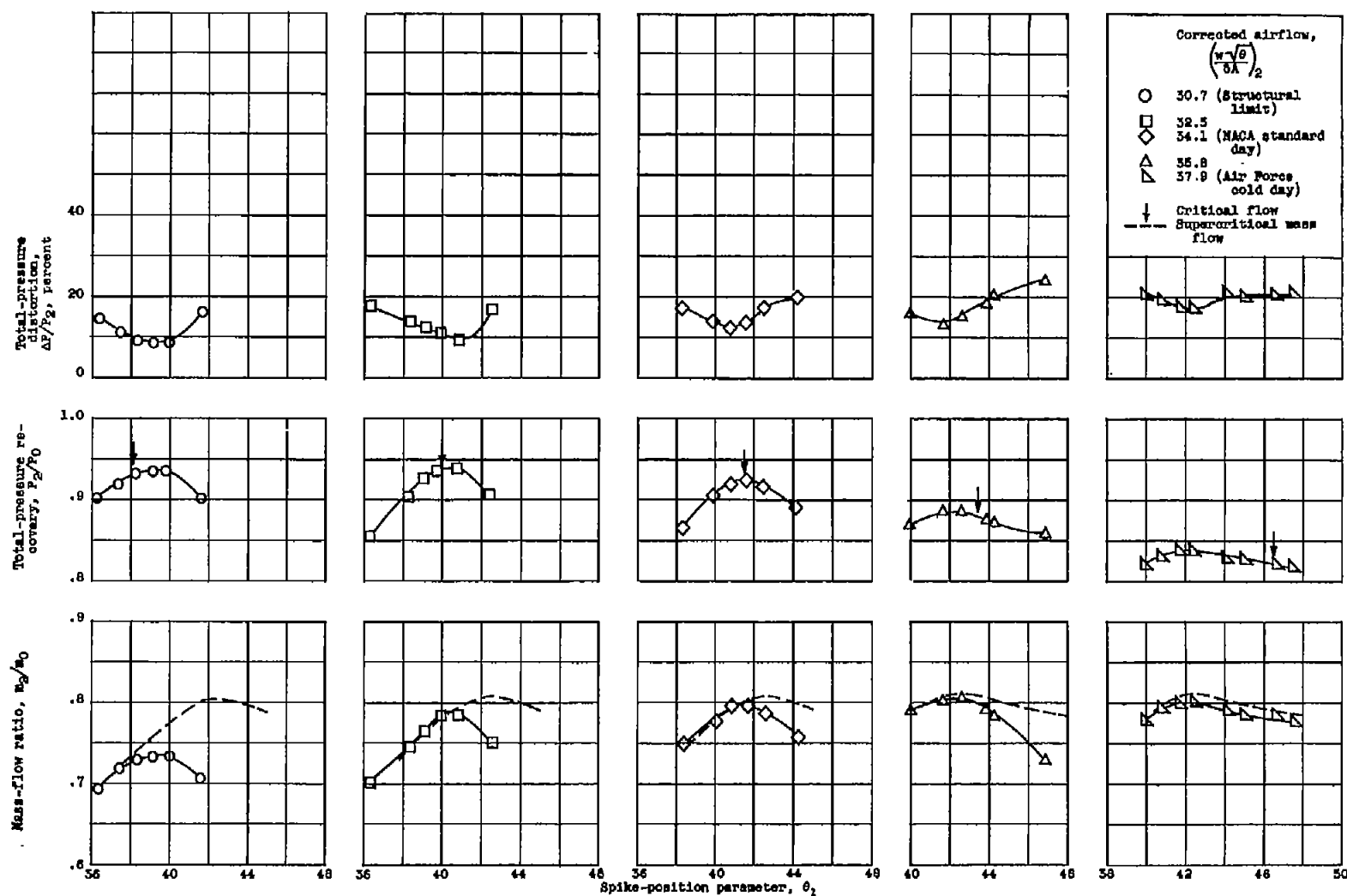
Figure 5. - Concluded. Inlet performance at free-stream Mach number of 2.0. Shock angle,  $42.6^\circ$ .

CONFIDENTIAL

CONFIDENTIAL

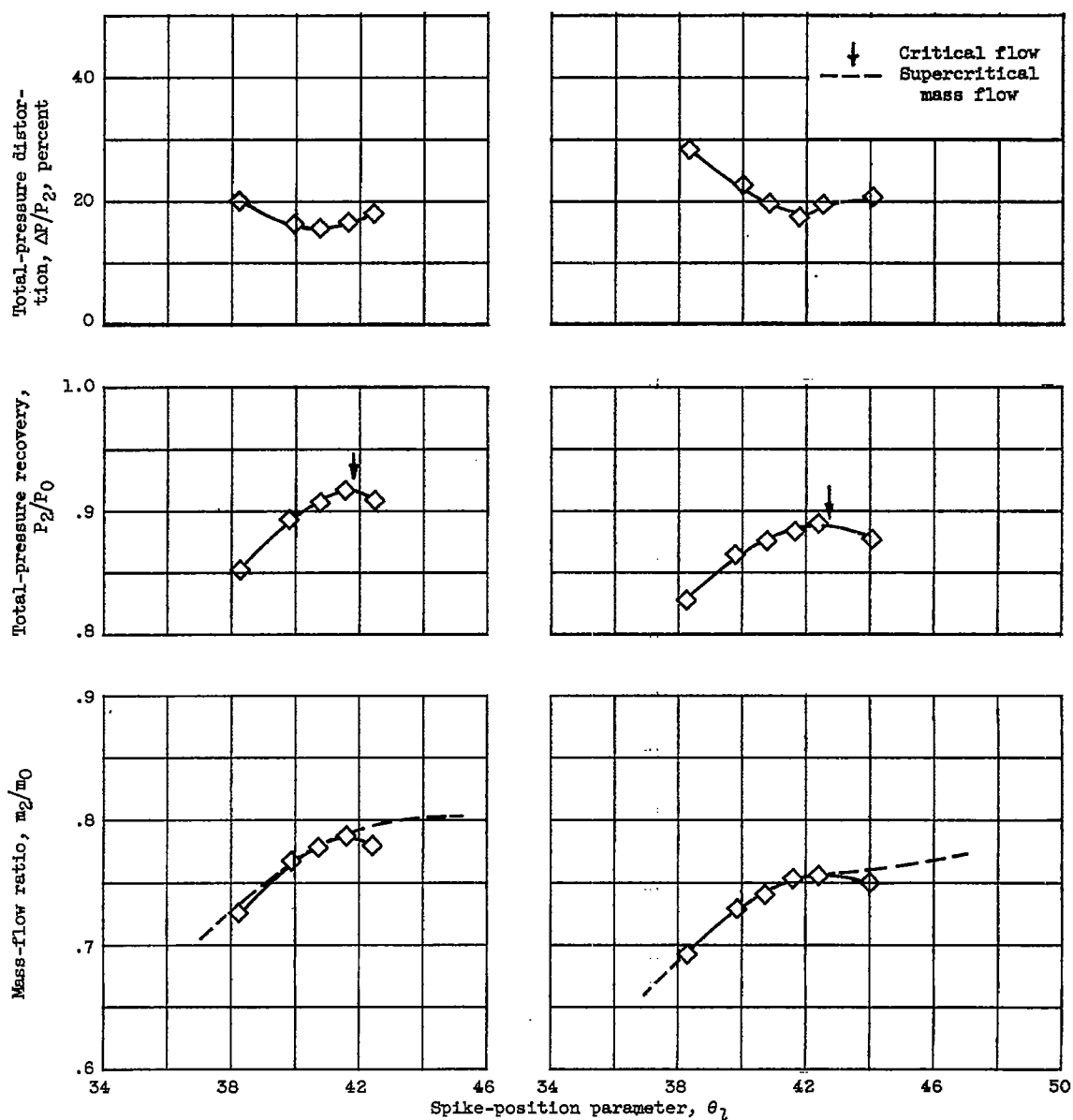
(a) Angle of attack,  $0^\circ$ .Figure 6. - Inlet performance at free-stream Mach number of 1.8. Shock angle,  $46.1^\circ$ .

CONFIDENTIAL

(b) Angle of attack,  $3^\circ$ .Figure 6. - Continued. Inlet performance at free-stream Mach number of 1.8. Shock angle,  $46.1^\circ$ .



CONFIDENTIAL

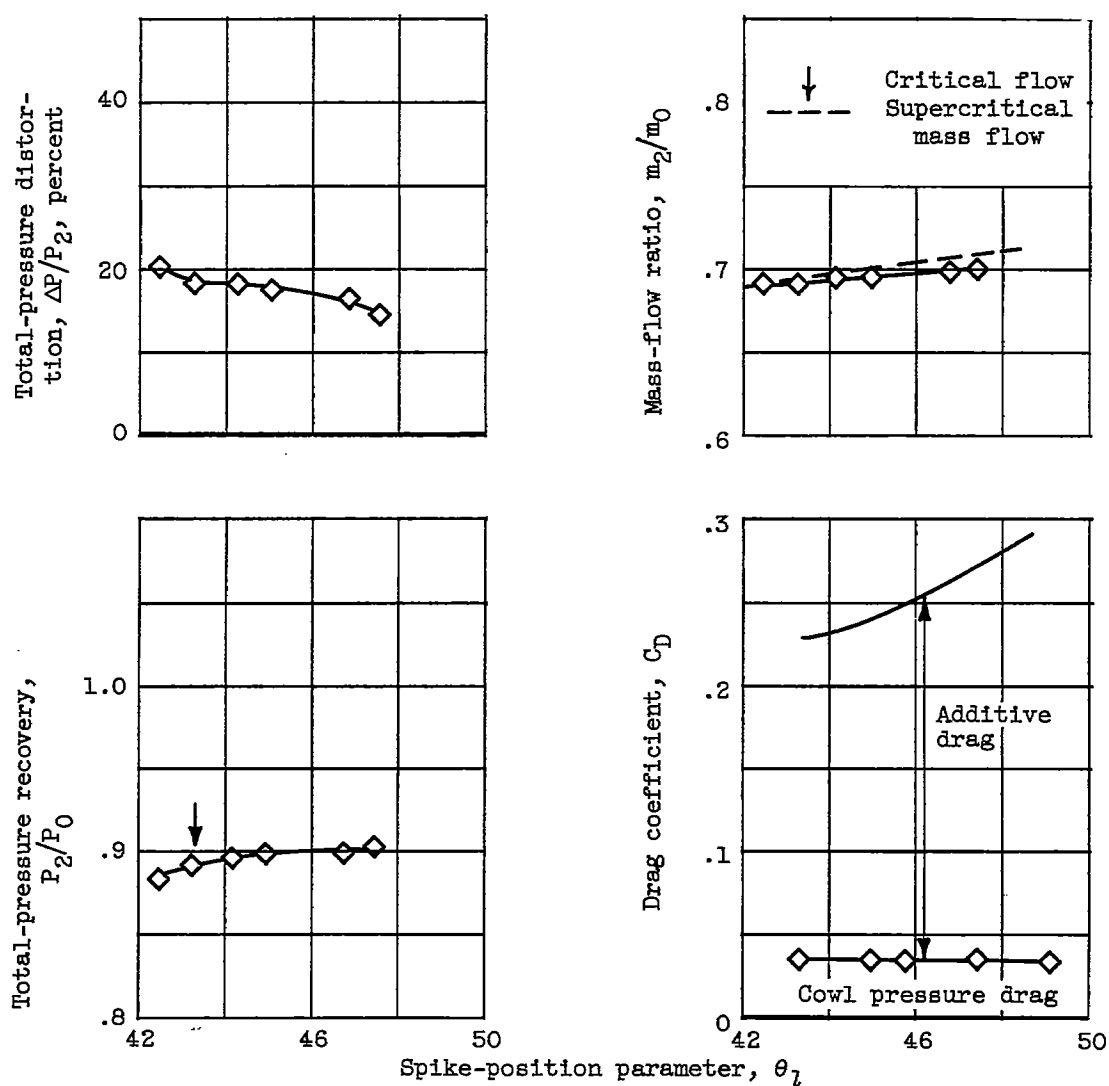


(c) Angle of attack,  $6^\circ$ ; corrected airflow, 34.1 (NACA standard day).

(d) Angle of attack,  $10^\circ$ ; corrected airflow, 34.1 (NACA standard day).

Figure 6. - Concluded. Inlet performance at free-stream Mach number of 1.8. Shock angle,  $46.1^\circ$ .

CONFIDENTIAL



(a) Angle of attack,  $0^\circ$ ; corrected airflow, 37.4 (NACA standard day).

Figure 7. - Inlet performance at free-stream Mach number of 1.5. Shock angle,  $54.9^\circ$ .

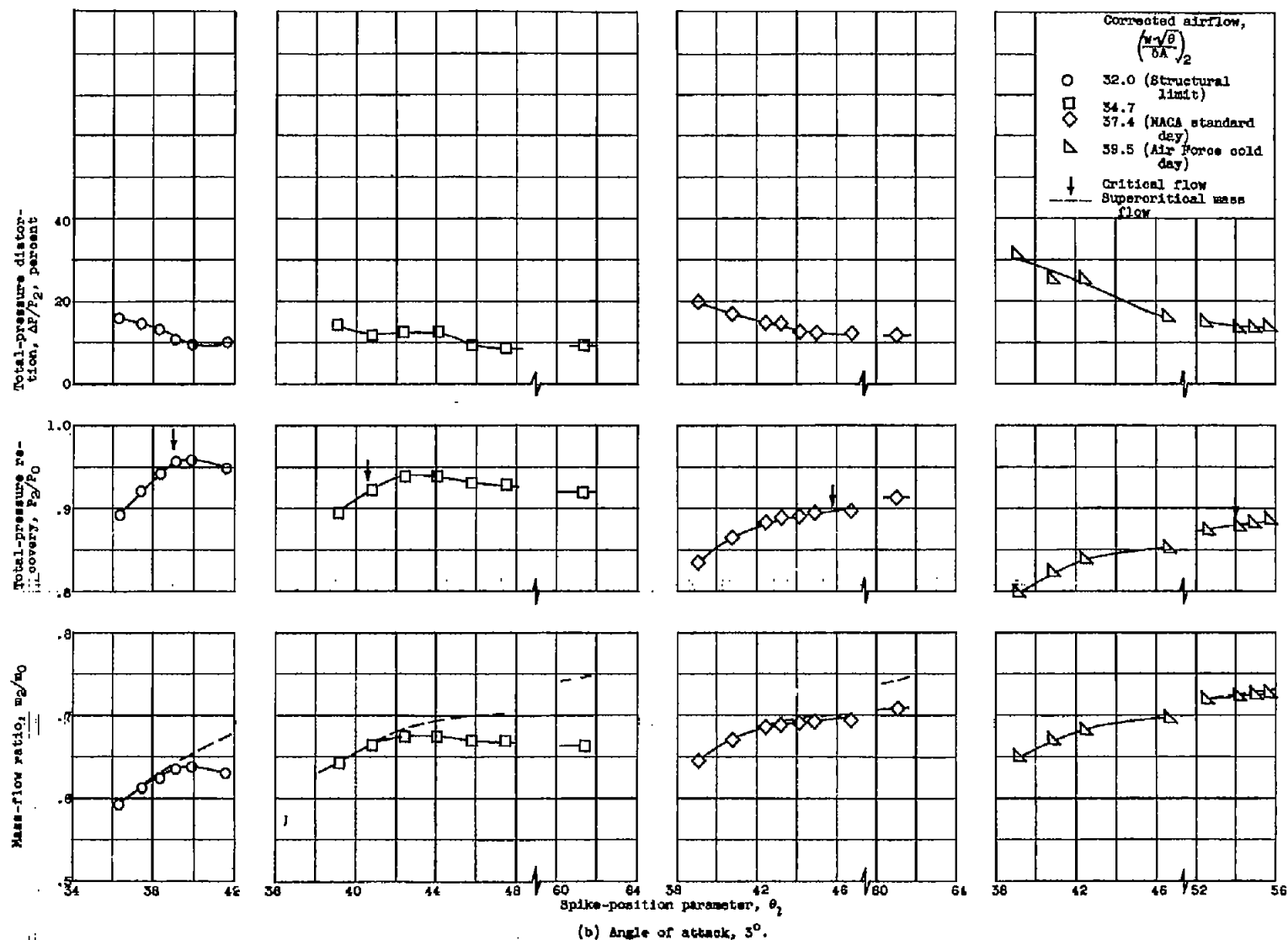
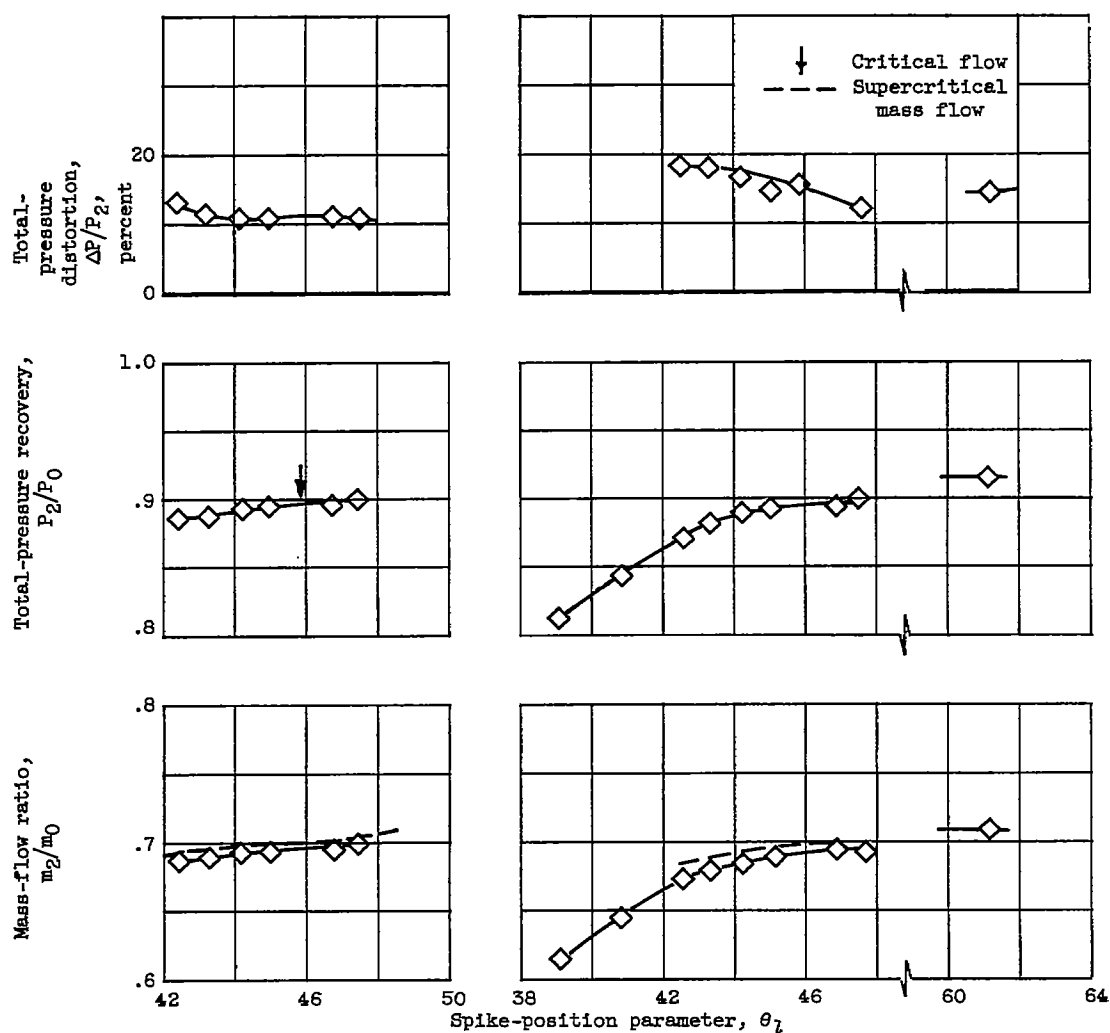


Figure 7. - Continued. Inlet-performance at free-stream Mach number of 1.5. Shock angle, 54.8°.



(c) Angle of attack,  $6^\circ$ ;  
corrected airflow,  
37.4 (NACA standard  
day).

(d) Angle of attack,  $10^\circ$ ; corrected airflow,  
37.4 (NACA standard day).

Figure 7. - Concluded. Inlet performance at free-stream Mach number of 1.5. Shock angle,  $54.9^\circ$ .

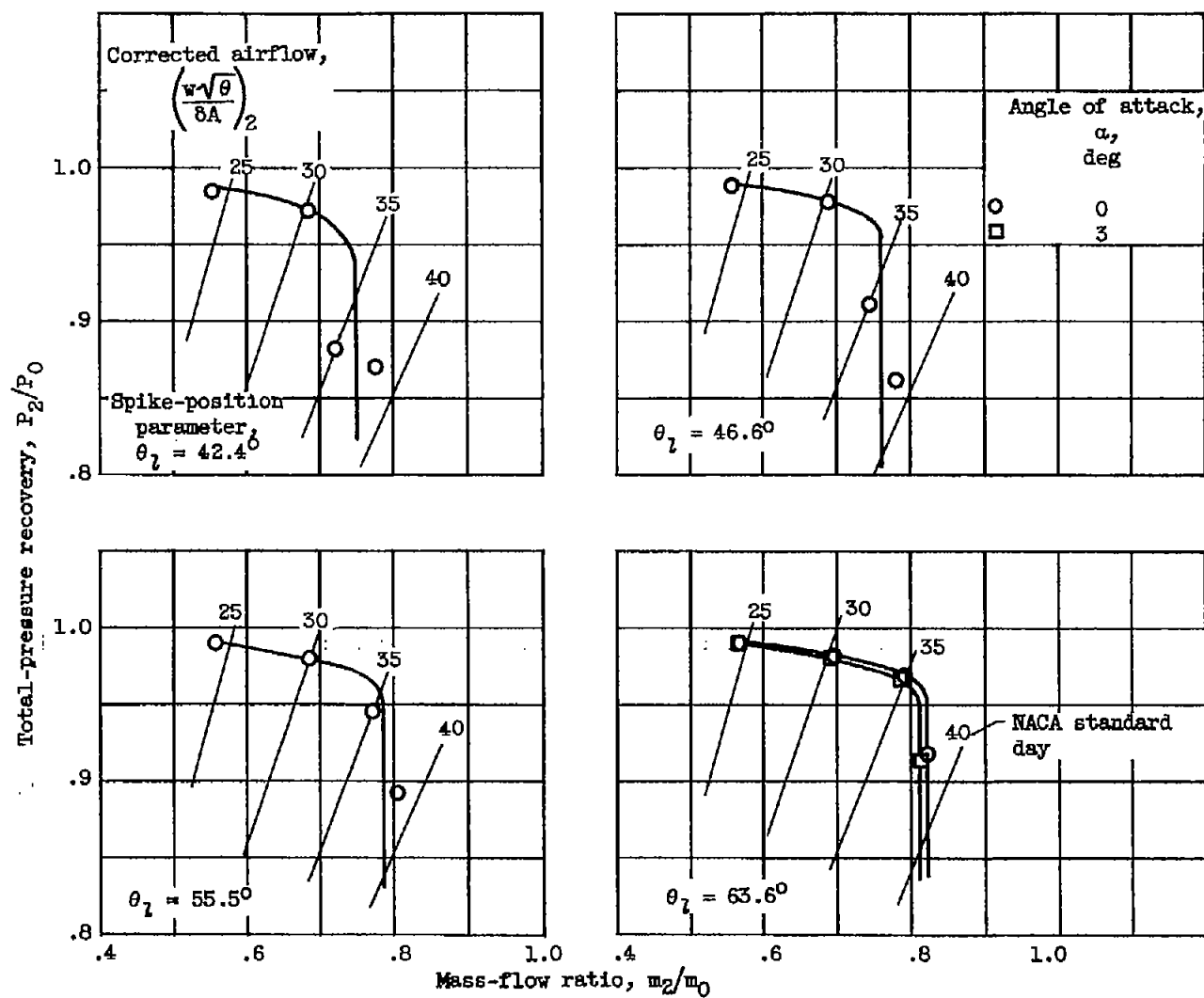
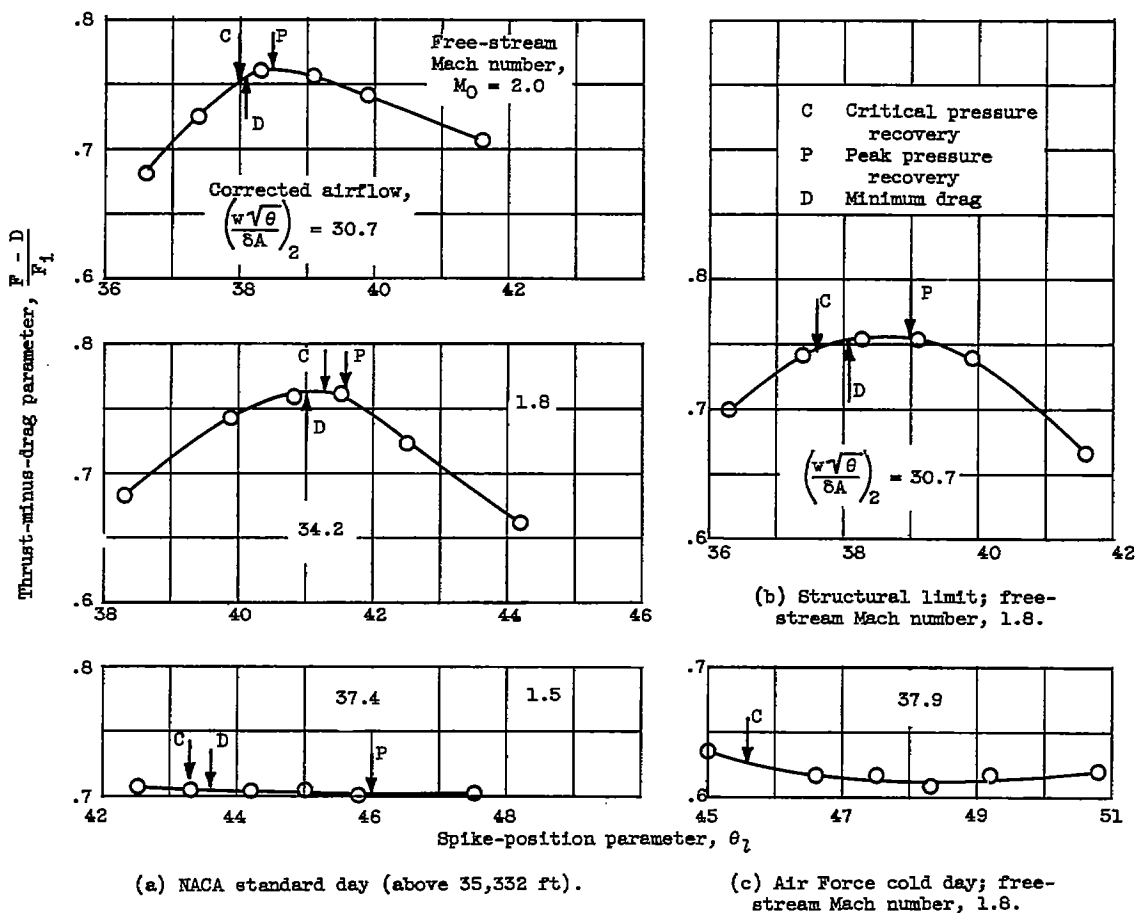


Figure 8. - Inlet performance at free-stream Mach number of 0.63.

Figure 9. - Net thrust performance; angle of attack,  $0^\circ$ .

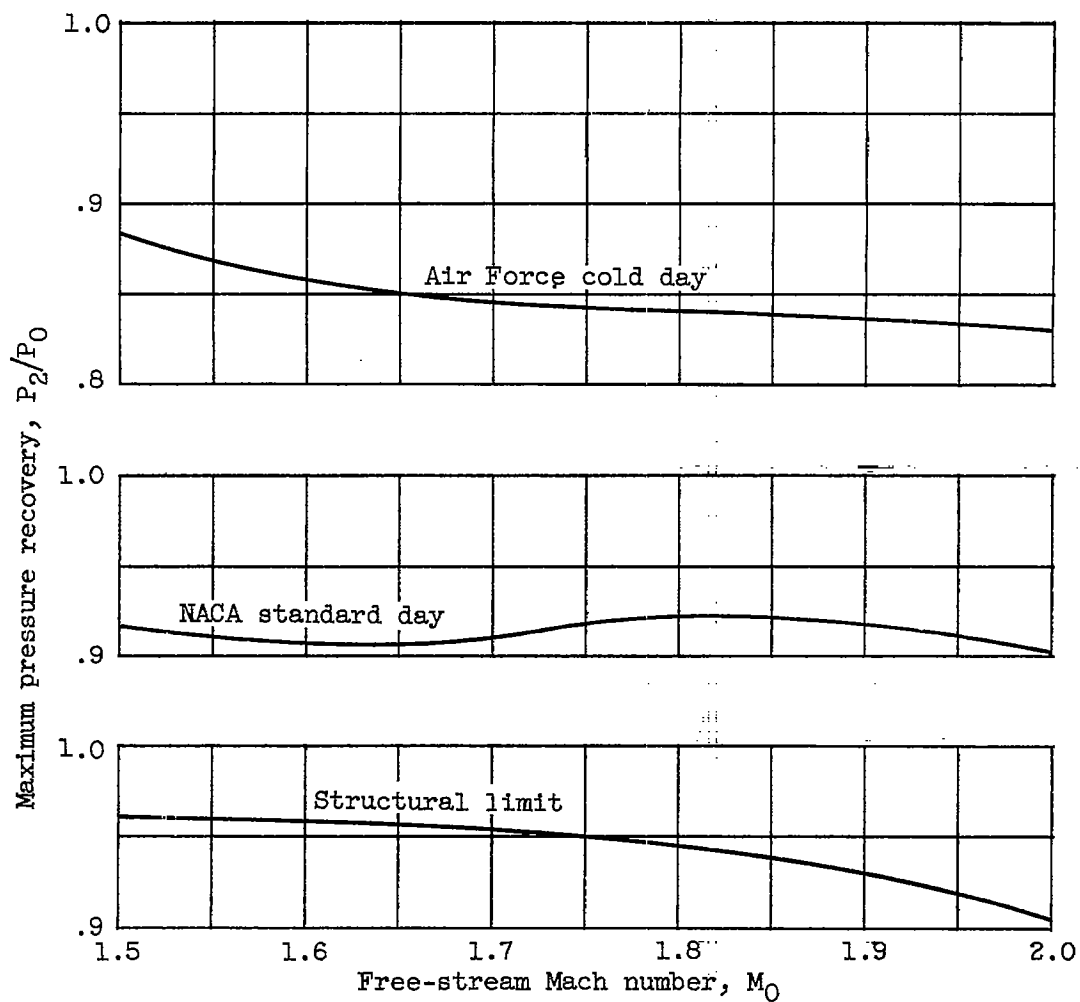


Figure 10. - Maximum pressure recovery; angle of attack,  $3^\circ$ .

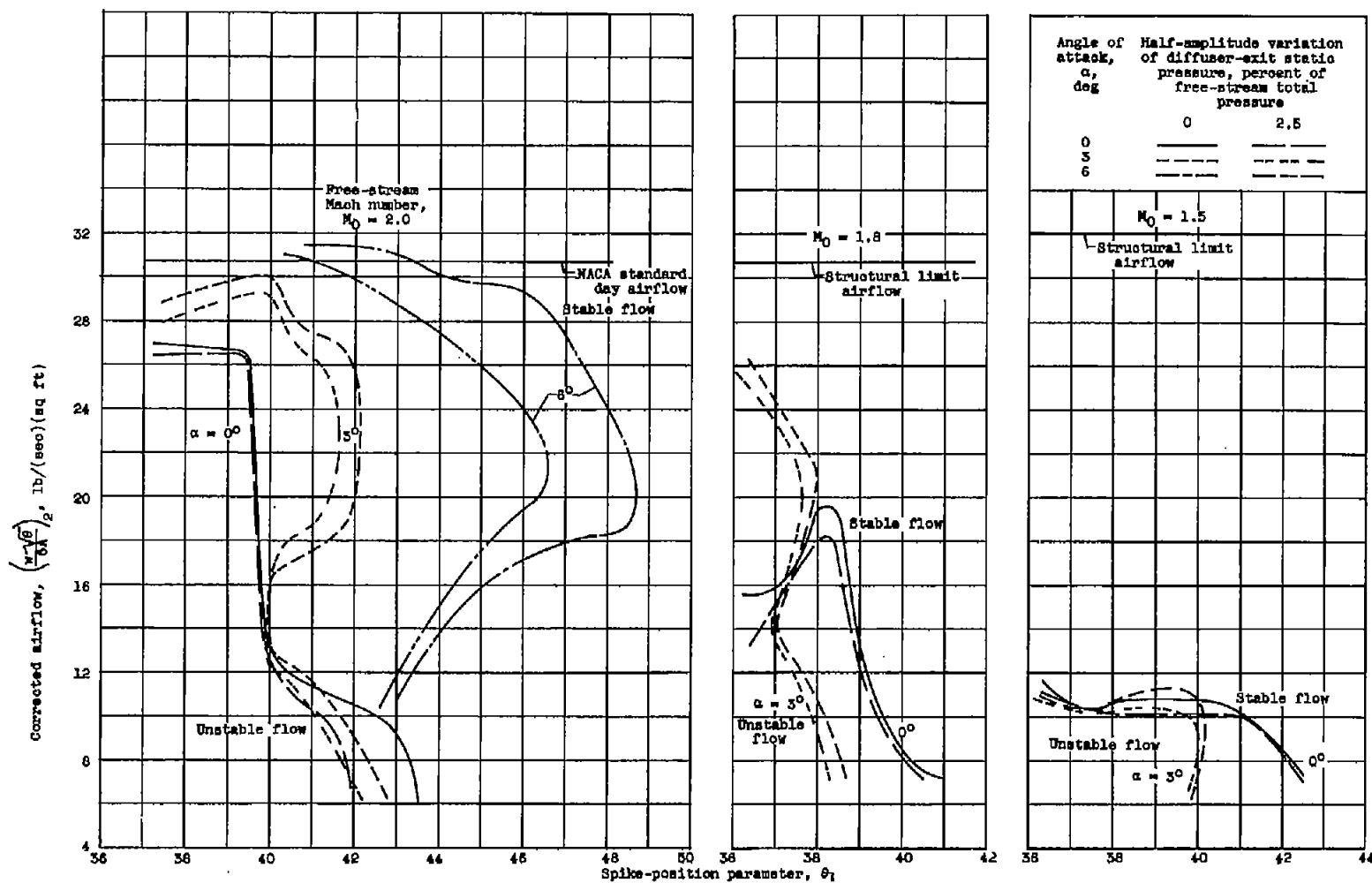


Figure 11. - Effect of spike translation on stability.





Free-stream Mach number,  
 $M_0 = 2.0$   
 Spike-position parameter,  
 $\theta_\gamma = 38.3^\circ$



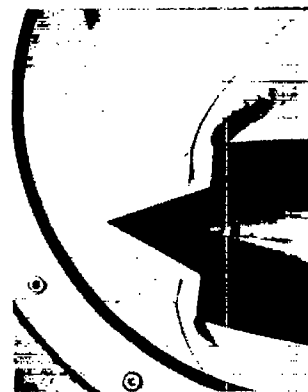
$M_0 = 2.0$   
 $\theta_\gamma = 38.3^\circ$



$M_0 = 2.0$   
 $\theta_\gamma = 42.5^\circ$



$M_0 = 1.8$   
 $\theta_\gamma = 38.3^\circ$



$M_0 = 1.8$   
 $\theta_\gamma = 41.6^\circ$



$M_0 = 1.8$   
 $\theta_\gamma = 46.6^\circ$



$M_0 = 1.5$   
 $\theta_\gamma = 39.1^\circ$



$M_0 = 1.5$   
 $\theta_\gamma = 45.9^\circ$



$M_0 = 1.5$   
 $\theta_\gamma = 54.1^\circ$

(a) Structural limit.

(b) NACA standard day.

(c) Air Force cold day.

Figure 12. - Schlieren photographs for spike positions near critical flow;  
 angle of attack,  $3^\circ$ .

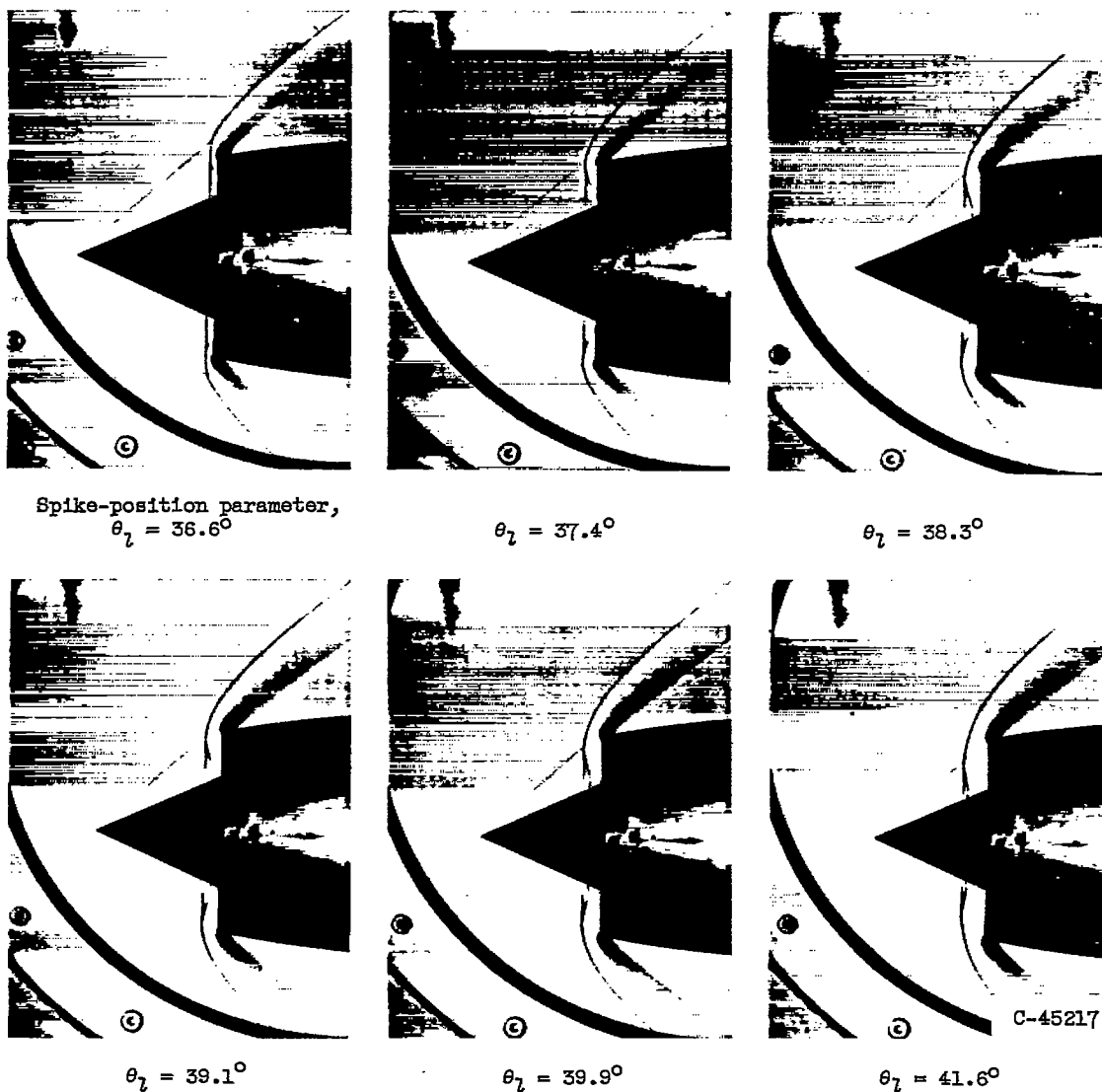
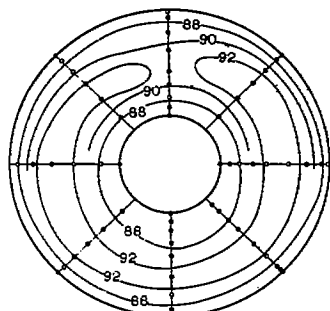
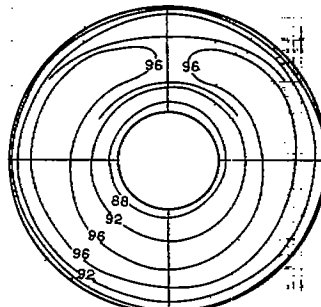


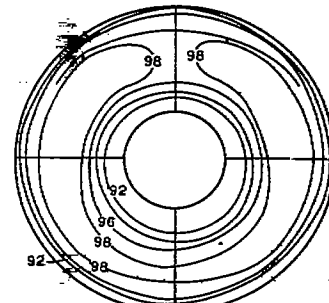
Figure 13. - Schlieren photographs showing variation of shock pattern with spike position. NACA standard day; free-stream Mach number, 2.0; angle of attack,  $0^\circ$ ; spike-position parameter for critical flow,  $38^\circ$ .



Distortion parameter,  $\Delta P/P_2 = 9.5$   
Free-stream Mach number,  $M_0 = 2.0$   
Spike-position parameter,  $\theta_1 = 38.3^\circ$

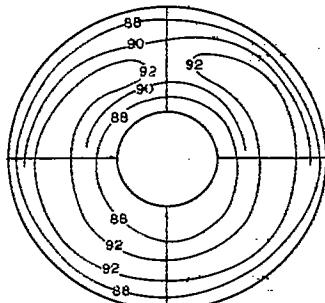


$\Delta P/P_2 = 9.5$   
 $M_0 = 1.8$   
 $\theta_1 = 38.3^\circ$

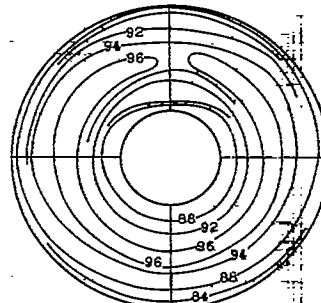


$\Delta P/P_2 = 11.0$   
 $M_0 = 1.5$   
 $\theta_1 = 39.1^\circ$

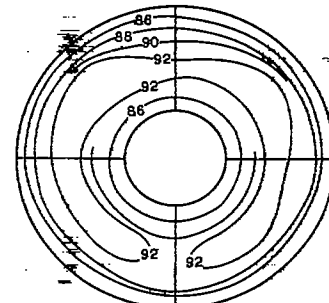
(a) Structural limit.



$\Delta P/P_2 = 9.5$   
 $M_0 = 2.0$   
 $\theta_1 = 38.3^\circ$

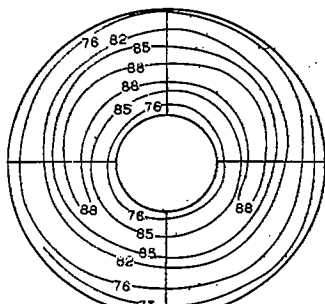


$\Delta P/P_2 = 13.8$   
 $M_0 = 1.8$   
 $\theta_1 = 41.6^\circ$

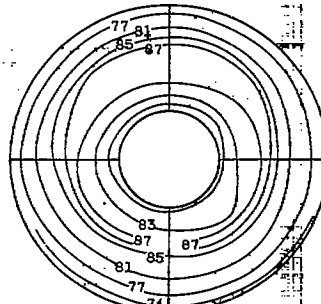


$\Delta P/P_2 = 12.0$   
 $M_0 = 1.5$   
 $\theta_1 = 45.9^\circ$

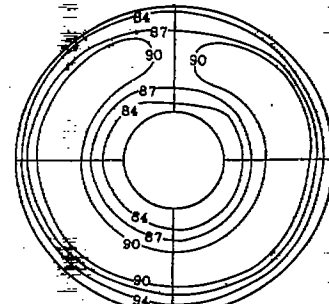
(b) NACA standard day.



$\Delta P/P_2 = 21.8$   
 $M_0 = 2.0$   
 $\theta_1 = 42.5^\circ$



$\Delta P/P_2 = 20.9$   
 $M_0 = 1.8$   
 $\theta_1 = 46.6^\circ$



$\Delta P/P_2 = 15.9$   
 $M_0 = 1.5$   
 $\theta_1 = 54.1^\circ$

(c) Air Force cold day.

Figure 14. - Total-pressure contours for spike positions near critical flow.  
Angle of attack,  $3^\circ$ .

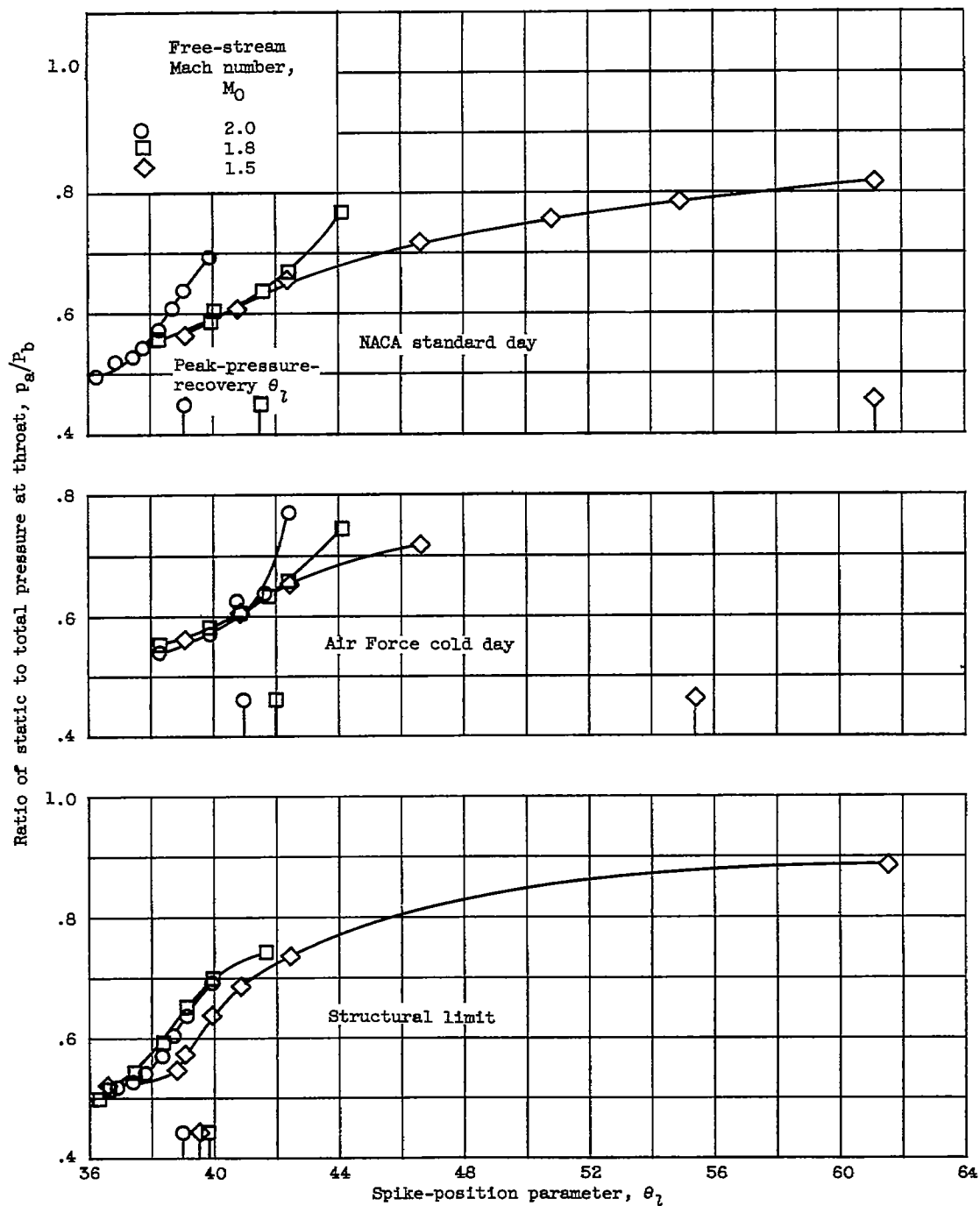
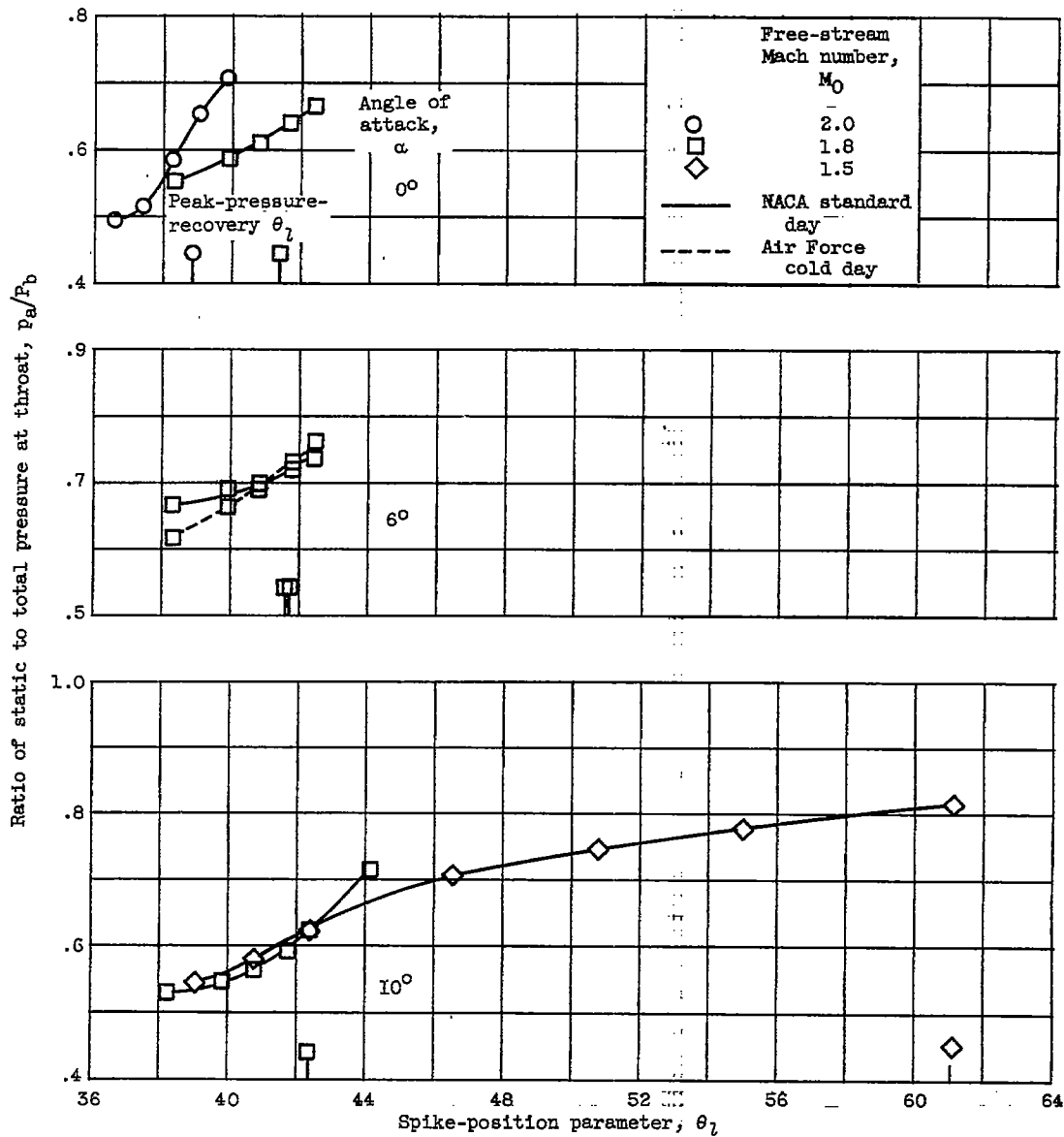
(a) Angle of attack,  $3^\circ$ .

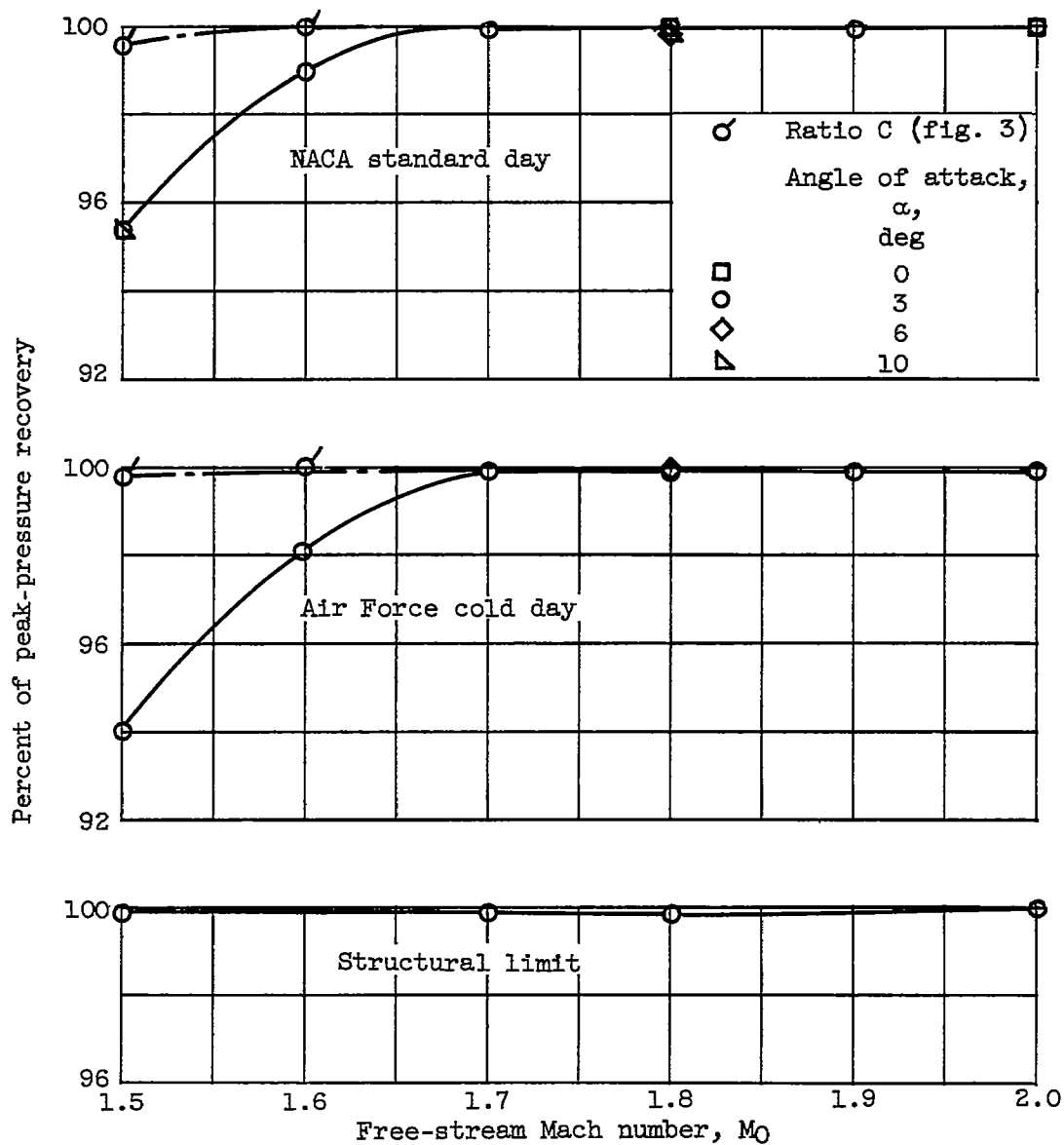
Figure 15. - Effect of spike position on throat pressure ratio (ratio A of fig. 3).

CONFIDENTIAL



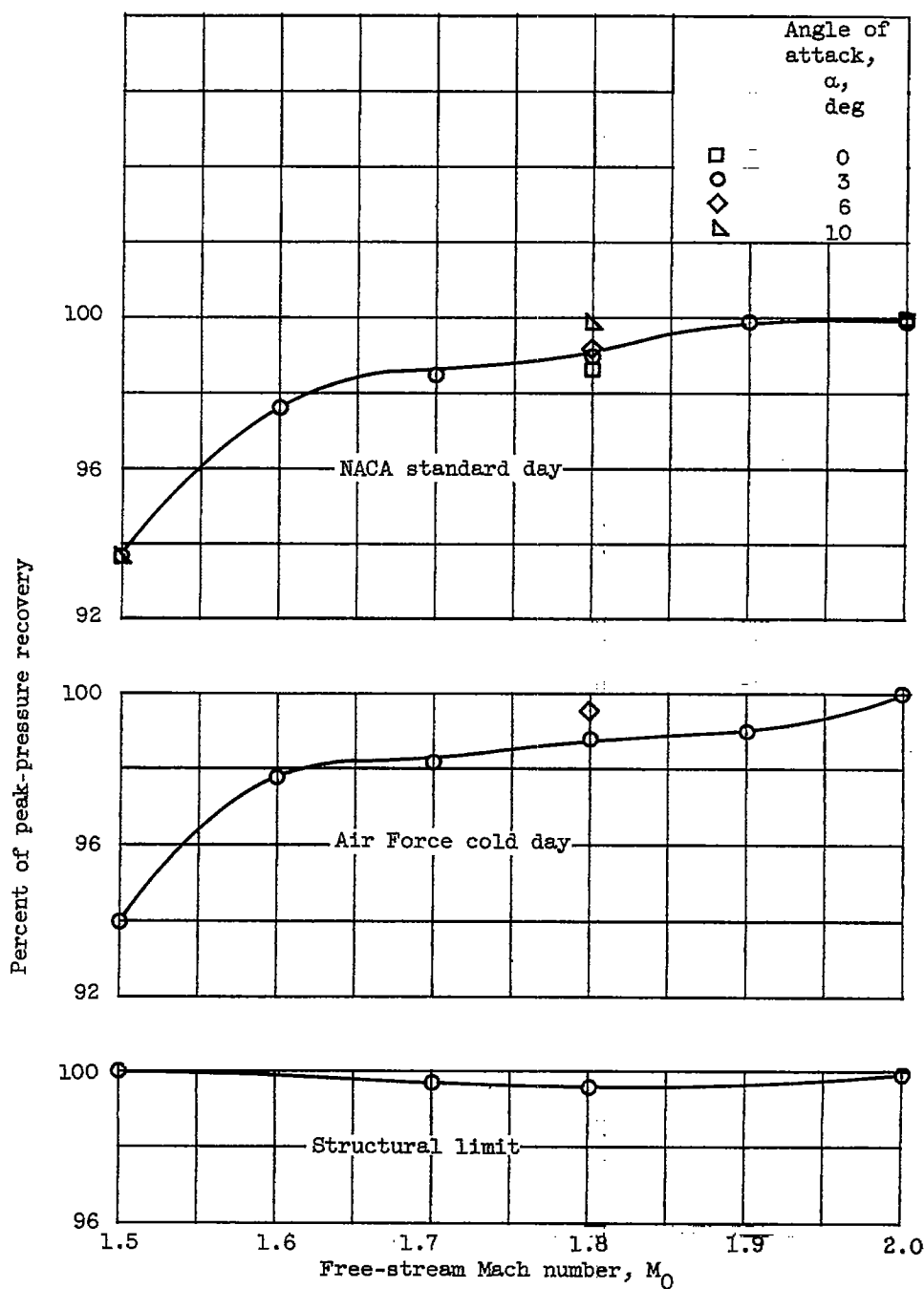
(b) Angles of attack, 0°, 6°, and 10°.

Figure 15. - Concluded. Effect of spike position on throat pressure ratio (ratio A of fig. 3).



(a) Pressure ratio, 0.63 ( $M_{local}$ , 0.84).

Figure 16. - Inlet performance using pressure ratio A (fig. 3) for control signal.



(b) Pressure ratio, 0.60 ( $M_{\text{local}}, 0.89$ ).

Figure 16. - Concluded. Inlet performance using pressure ratio A (fig. 3) for control signal.

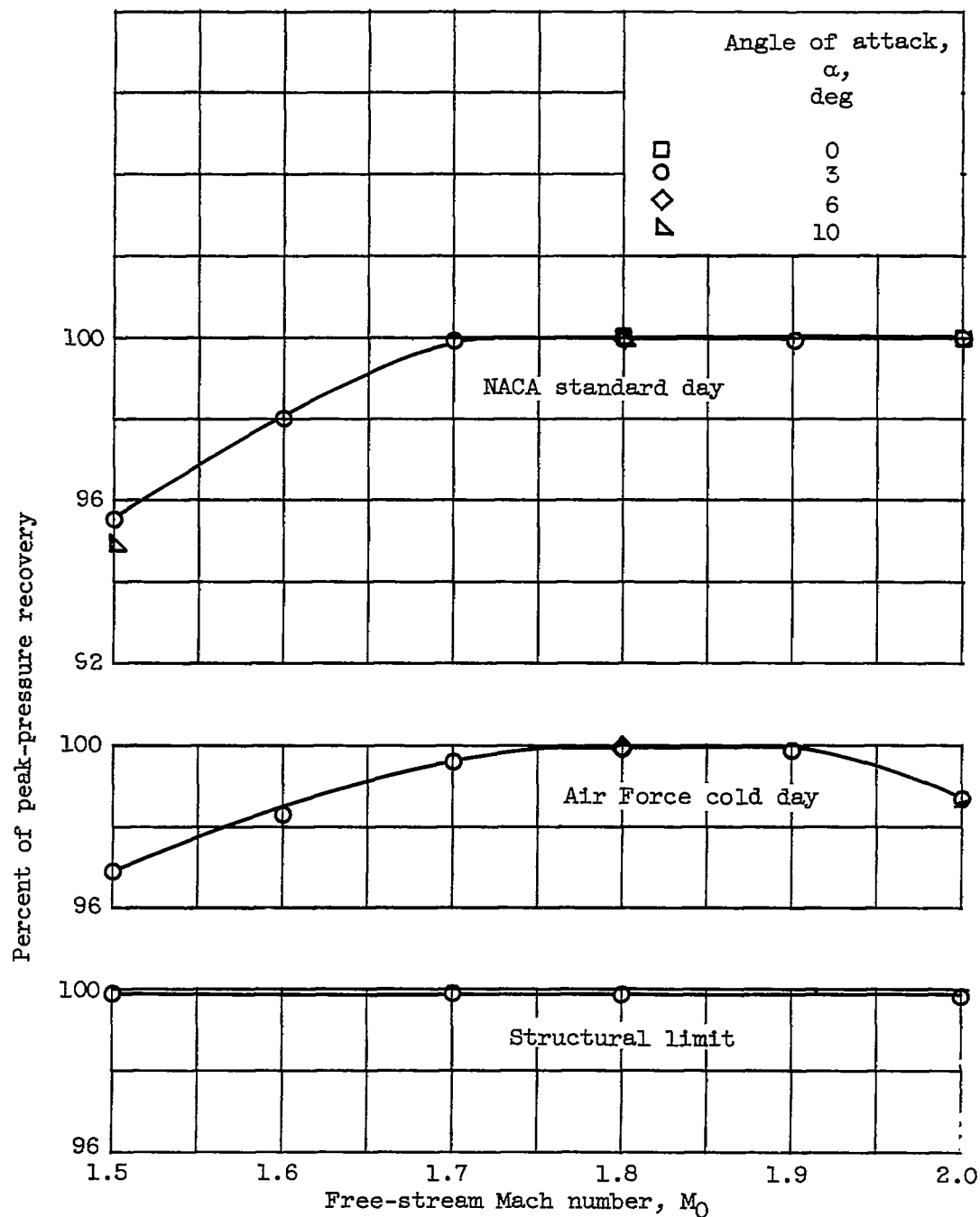


Figure 17. - Inlet performance using pressure ratio B (fig. 3) for control signal. Ratio value, 0.61; local Mach number, 0.87.



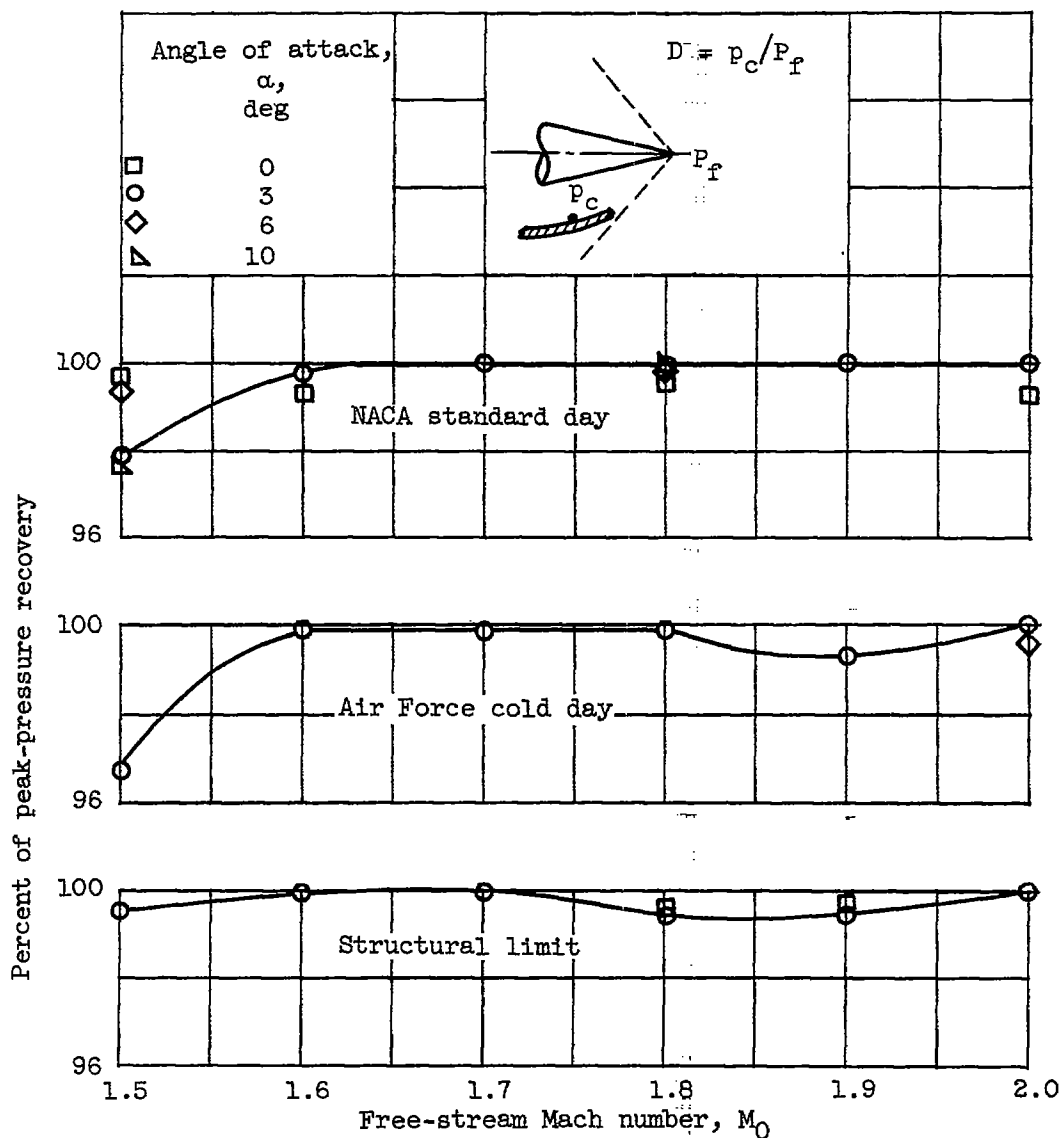


Figure 18. - Inlet performance using pressure ratio  $D$  (fig. 3) for control signal. Ratio value, 0.70.

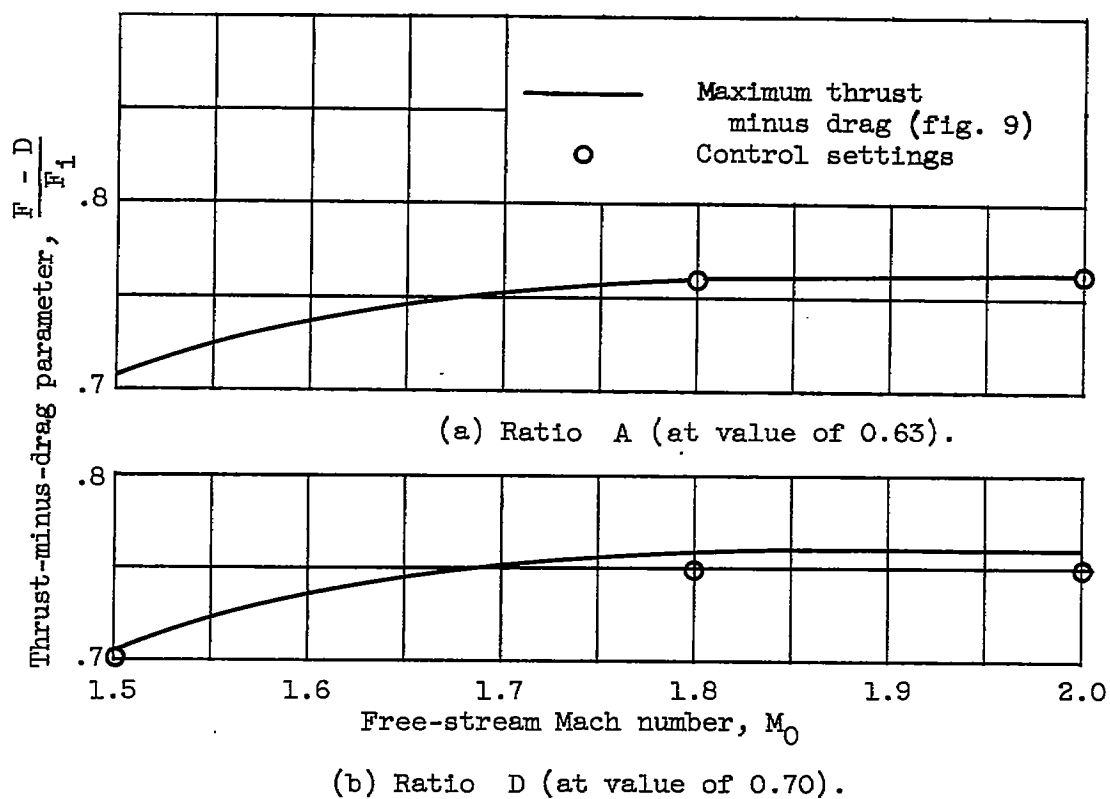


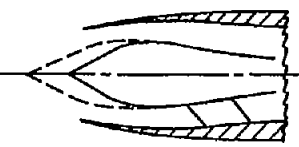
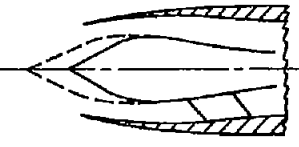
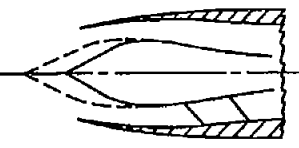
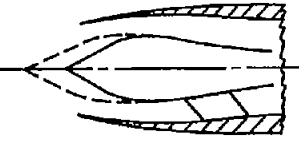
Figure 19. - Thrust-minus-drag performance with ratios A and D (fig. 3). NACA standard day; angle of attack,  $0^\circ$ .



# CONFIDENTIAL

NOTES: (1) Reynolds number is based on the diameter of a circle with the same area as that of the capture area of the inlet.

(2) The symbol \* denotes the occurrence of buzz.

Report and facility	Description			Test parameters				Test data				Performance		Remarks
	Configuration	Number of oblique shocks	Type of boundary-layer control	Free-stream Mach number	Reynolds number $\times 10^{-6}$	Angle of attack, deg	Angle of yaw, deg	Drag	Inlet-flow profile	Discharge-flow profile	Flow picture	Maximum total-pressure recovery	Maximum mass-flow ratio	
CONFID. RM E57D15 Lewis 8-by 8-ft super-sonic wind tunnel		1	None	2.0	3.2	0,3,6,10	0	✓	No	✓	✓	0.90	0.89	Translating spike, blunt lip, overcontracted for range of spike positions Pressures measured near throat were evaluated as spike control signals
				1.8	3.2	0,3,6,10	0	✓	No	✓	✓	.945	.81	
				1.5	3.2	0,3,6,10	0	✓	No	✓	✓	.96	.74	
CONFID. RM E57D15 Lewis 8-by 8-ft super-sonic wind tunnel		1	None	2.0	3.2	0,3,6,10	0	✓	No	✓	✓	0.90	0.89	Translating spike, blunt lip, overcontracted for range of spike positions Pressures measured near throat were evaluated as spike control signals
				1.8	3.2	0,3,6,10	0	✓	No	✓	✓	.945	.81	
				1.5	3.2	0,3,6,10	0	✓	No	✓	✓	.96	.74	
CONFID. RM E57D15 Lewis 8-by 8-ft super-sonic wind tunnel		1	None	2.0	3.2	0,3,8,10	0	✓	No	✓	✓	0.90	0.89	Translating spike, blunt lip, overcontracted for range of spike positions Pressures measured near throat were evaluated as spike control signals
				1.8	3.2	0,3,8,10	0	✓	No	✓	✓	.945	.81	
				1.5	3.2	0,3,8,10	0	✓	No	✓	✓	.96	.74	
CONFID. RM E57D15 Lewis 8-by 6-ft super-sonic wind tunnel		1	None	2.0	3.2	0,3,8,10	0	✓	No	✓	✓	0.90	0.89	Translating spike, blunt lip, overcontracted for range of spike positions Pressures measured near throat were evaluated as spike control signals
				1.8	3.2	0,3,8,10	0	✓	No	✓	✓	.945	.81	
				1.5	3.2	0,3,8,10	0	✓	No	✓	✓	.96	.74	

## Bibliography

These strips are provided for the convenience of the reader and can be removed from this report to compile a bibliography of NACA inlet reports. This page is being added only to inlet reports and is on a trial basis.

CONFIDENTIAL